

# FLUORESCENCE READOUTS OF BIOCHEMISTRY IN LIVE CELLS AND ORGANISMS

ROGER Y. TSIEN, PHD

This chapter discusses the most common general principles by which fluorescence is used to measure important biochemical species or monitor biochemical pathways in living cells, tissues, and organisms. Fluorescence is a uniquely powerful and complex imaging modality because it combines high spatial resolution, time resolution, sensitivity, and spectroscopic modulation. Classical microscopy permits spatial resolution down to about 200 nm, but single fluorescent particles can now be localized down to  $\sim 1$  nm precision,<sup>1-3</sup> and spectroscopic techniques, such as fluorescence resonance energy transfer (FRET), can report yet smaller distance changes. The time resolution of fluorescence intrinsically extends at least to the nanosecond domain, that is, far faster than most biochemical events. Fluorescence recordings of live cell physiology typically range from nanoseconds to many hours (Figure 1A). In cell-free systems, single fluorescent molecules can be reliably detected,<sup>4,5</sup> which for many applications is the ultimate sensitivity limit. Finally, fluorescence can be usefully modulated by a wide variety of molecular mechanisms. This environmental sensitivity stands in starkest contrast to radioactive decay, which is completely indifferent to the chemical environment. Of course, fluorescence also has some fundamental limitations. Strongly fluorescent tags are full-sized molecules in their own right, so attachment to a biological molecule of interest can perturb the latter significantly. Strong illumination of fluorophores eventually bleaches them and can also damage surrounding molecules and cells. Fluorescence imaging inside most intact tissues and organisms rapidly loses spatial resolution and sensitivity as depths increase from tens of microns to millimeters or centimeters (Figure 1B). In most systems from live cells to intact organisms, endogenous background fluorescence (autofluorescence), rather than instrumental sensitivity,

determines the minimum detectable concentration of exogenous fluorophores.

Space limitations forbid detailed explanations of the basic physical principles of fluorescence or of sophisticated biophysical techniques mainly applicable to purified molecules *in vitro*. Standard textbooks should be consulted for such topics.<sup>6</sup> I first discuss the general mechanisms by which fluorescence can report biological signals in live cells and organisms. Then I review how some of the more important pathways have actually been imaged. Again because of space limitations, I mainly cite recent reviews, rather than describe biological results in detail or credit all the original pioneers.

## MAJOR MECHANISMS FOR FLUORESCENCE RESPONSES IN LIVE CELLS AND ORGANISMS

### Fluorophore as Spectroscopically Passive Tag for Macromolecule of Interest

Many applications of fluorescence make no use of its potential environmental sensitivity. Instead, the fluorophore is attached to a molecule of interest merely to make the latter visible and trackable. Such tagging is required because few biologically relevant molecules have useful intrinsic fluorescence. Among the exceptions<sup>7</sup> are reduced pyridine nucleotides (NADH and NADPH), flavins, tetrapyrroles, such as protoporphyrin IX and chlorophyll, and aging-related pigments, such as lipofuscins. Many proteins are somewhat fluorescent at ultraviolet (UV) wavelengths due to their tryptophan content, but such fluorescence is mainly useful for studying purified proteins rather than intact cells because the excitation wavelengths ( $\sim 300$  nm) are phototoxic and too short for

most microscopes and because no one protein stands out sufficiently from all the others.

### Exogenous Added Dyes, Peptides, Proteins

Traditionally, peptides and proteins are tagged *in vitro* by reacting free amino or thiol groups of the purified macromolecule with reactive derivatives of fluorescent dyes. Isothiocyanates and N-hydroxysuccinimide (NHS) esters are probably the most popular amine-reactive derivatives, whereas maleimides and iodoacetyl groups are the dominant thiol-reactive derivatives. The most common fluorophores are xanthenes (fluoresceins and rhodamines)

for emission maxima of up to about 600 nm, whereas indolenine cyanines start around 550 nm and dominate above 600 nm. Many other fluorophores have advantages for specific applications and are tabulated in catalogs.<sup>8</sup> Although longer wavelengths are usually biologically advantageous because of deeper penetration and reduced background fluorescence and phototoxicity, the corresponding fluorophores are chemically less convenient, being less rugged, less water-soluble, and generally less tractable than their cousins operating at shorter wavelengths. The fundamental limitations on this approach are the need to isolate and purify reasonable quantities of the starting macromolecule, to devise a labeling protocol that confers sufficient fluorescence without destroying the essential biochemical properties, and to reintroduce the labeled macromolecule to the appropriate location in the cell or organism, which is particularly challenging if that location is intracellular.

### Fluorescent Proteins

Protein labeling and *in vivo* fluorescence have been revolutionized by the discovery, cloning, and mutagenic improvement of natural proteins with strong visible fluorescence.<sup>9-11</sup> Thus far, all such fluorescent proteins (FPs) have originated from marine coelenterates, such as jellyfish and corals, are cylindrical 11-stranded  $\beta$  barrels of ~2.4 nm diameter and 4 nm length, and contain at least 200 amino acids. The light-absorbing unit or chromophore is a hydroxybenzylideneimidazolinone, generated by spontaneous cyclization and autoxidation of a few amino acids on a helix running up the center of the cylinder. Many variations of chromophore structure (Figure 2) have been generated by ecological diversification and artificial reengineering and are responsible for a wide range in colors. The crucial advantage of FPs is their genetic encodability, so that cells expressing the gene encoding the FP become fluorescent. In-frame fusion of the FP gene with the gene for the protein of interest generates a chimeric protein *in situ*, which hopefully (and often actually) functions like the native protein except that it is fluorescent. Thus, the protein never has to be purified *in vitro*, the location of the tag within the primary sequence is accurately specified, and the normal biosynthetic machinery of the cell can be used to target the chimera to virtually any desired location. After much engineering, well-behaved FPs<sup>9-11</sup> are now available with excitation maxima from about 380 to 598 nm, emission maxima from 440 to 650 nm, fairly good resistance to photobleaching and other environmental factors, very little phototoxicity, and lack of oligomerization. Obligate dimer or tetramer formation is a feature

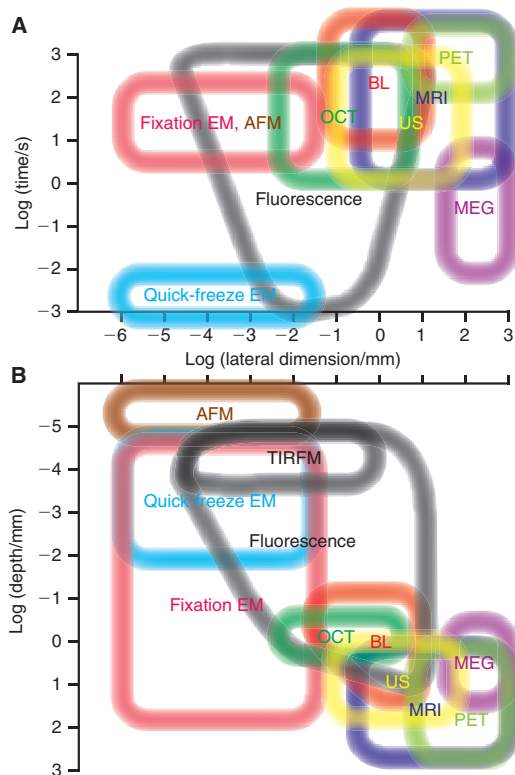


**Figure 1. Comparison of the lateral dimensions, time scales, and depth penetrations of major imaging modalities.** Note that all scales are logarithmic and that all boundaries are fuzzy and can be breached by unusual examples or technological improvements. *A*, Time scales vs lateral dimensions. *B*, Depth penetration vs lateral dimensions. EM, electron microscopy; AFM, atomic force microscopy; OCT, optical coherence tomography; BL, bioluminescence; US, ultrasound; MRI, magnetic resonance imaging; PET, positron emission tomography; MEG, magnetoencephalography; TIRFM, total internal reflection fluorescence microscopy. The boundary for each modality roughly matches the hue of its label.

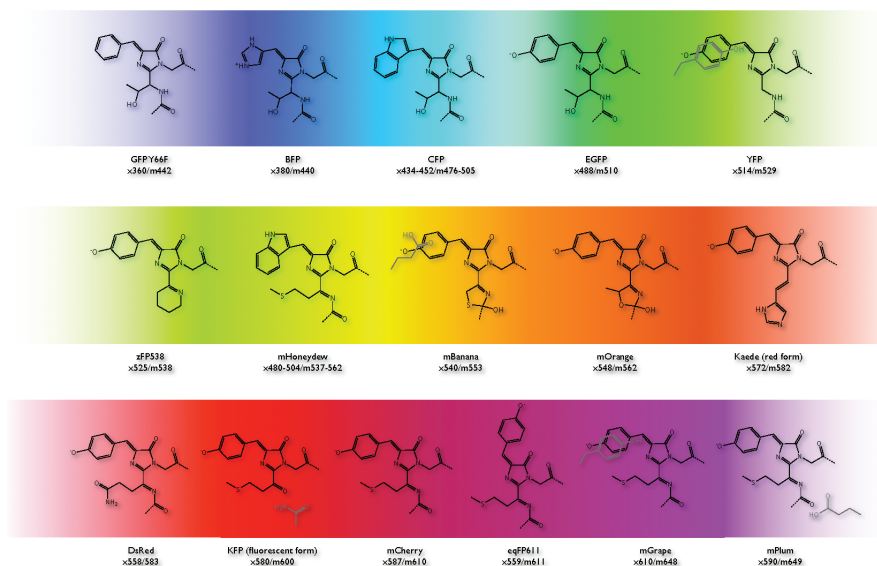
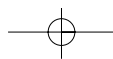
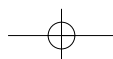


**Figure 2. Structures of the chromophores of representative fluorescent proteins, ranging from the shortest to the longest emission wavelengths.** Side chains that significantly influence the fluorescence are shown in gray.

of many wild-type FPs, especially the longer-wavelength representatives from corals.<sup>12</sup> Such oligomerization can be problematic when the FP is fused to a protein of interest because the latter is forced to join in the aggregation, which can readily cause mistrafficking, precipitation, or toxicity.<sup>13</sup> Oligomerization is less frequently a problem when the FP is left unfused simply to mark whole cells or tissues, but it may explain why several attempts to make transgenic mice expressing tetrameric red FPs (DsRed varieties) failed.<sup>14-16</sup> This problem was eventually solved by the introduction of monomeric or tandem-dimeric mutants of red FPs.<sup>13,17,18</sup> (A tandem dimer is a concatenation of two copies of the protein such that the dimeric protein-protein interaction is satisfied intramolecularly). Even the original jellyfish green fluorescent protein (GFP) and all color variations are weakly dimeric ( $K_d \sim 0.1$  mM)<sup>19,20</sup> unless the dimer interface has been deliberately destroyed by mutagenesis. This weak association can cause problems when monitoring protein-protein interactions, especially at high local concentrations or when the proteins are anchored to membranes.<sup>20,21</sup> The above discussion has focused on FPs as passive tags, but FP variants have also been evolved in which the fluorescence spontaneously changes color or can be usefully switched on or off by different wavelengths of light or environmental factors (see sections “Single FP: Perturbation of Chromophore Protonation” and “Protein Trafficking and Degradation”).

Of course, FPs have their own limitations. The most fundamental are that their size cannot be significantly reduced, that they require some  $O_2$  to generate their internal fluorophores, and that  $H_2O_2$  is a stoichiometric by-product of these reactions.<sup>9,22</sup> An early claim of a half-sized FP proved to be an artifact.<sup>23</sup> The  $O_2$  dependence should be kept in mind when using FPs as readouts under hypoxic conditions, but fortunately the autoxidation can proceed at quite low partial pressures of  $O_2$  ( $\sim 0.1$  ppm<sup>24</sup> or about 3  $\mu M$ ), and sometimes the readout can be postponed until after  $O_2$  can be readmitted to finish the maturation process.<sup>25</sup> Current shortcomings that might be ameliorated by further protein engineering include the lack of bright FPs with really long wavelengths (excitation maxima  $> 600$  nm to avoid the hemoglobin absorbance edge, emission maxima  $> 650$  nm) and photostability that is still not as good as the best small molecules or quantum dots.

**Translocation Assays**<sup>26,27</sup> Intracellular signaling pathways often involve translocation of a transducer protein from one subcellular compartment to another, for example, from cytosol to the plasma membrane or into the nucleus, or the reverse. Examples include recruitment of protein kinase C from cytosol to the plasma membrane by generation of  $Ca^{2+}$  and diacylglycerol, recruitment of  $\beta$ -arrestin from cytosol to activated G-protein-coupled receptors, release of pleckstrin homology domains from plasma



membrane to cytosol upon hydrolysis of phosphatidylinositol-4,5-bisphosphate to inositol 1,4,5-trisphosphate (Ins(1,4,5)P<sub>3</sub>), translocation of the nuclear factor of activated T cells (NF-AT) into the nucleus upon dephosphorylation by calcineurin, etc. Such activation steps can usually be monitored simply by fusing the translocating protein to an FP and imaging the subcellular distribution of the chimera.<sup>26,27</sup> Such assays are usually simple to establish and quite robust, though rarely calibrated in terms of the concentration of triggering ligand. Their disadvantages are that high spatial resolution is required and that the speed of response may be limited by diffusion kinetics.

### Genetically Targeted Small Molecules

For many purposes, it would be desirable to combine genetic targeting with the phenotypic versatility and small size of man-made dyes and probe molecules.<sup>28,29</sup> The most compact products would be achieved by hijacking specific stop codons to encode single unnatural (eg, fluorescent) amino acids. This requires reengineering transfer RNAs (tRNA) and tRNA-synthetases to incorporate the desired unnatural amino acid. Also, the hijacked codon has to be inserted into the relevant mRNA, but the concern remains that other endogenous mRNAs that happen to use that stop codon will translate into proteins also incorporating the unnatural amino acid plus C-terminal extensions encoded by previously untranslated 3' sequences. Therefore, this strategy has not yet progressed enough to be relied upon for molecular imaging of intact cells or organisms, though this may well change due to active current research.<sup>30</sup> The next step up in size is to devise a short (< 20 aa) peptide sequence that can be incorporated into the protein of interest and that can be labeled in situ with small organic molecules. The earliest example was a tetracysteine motif, -CCXXCC-, which can be labeled inside live cells with membrane-permeant dyes containing two arsenic atoms at the right spacing to plug into the two pairs of sidechain thiol groups.<sup>31</sup> Antidotes that prevent the biarsenical dye from poisoning endogenous proteins with cysteine pairs need to be co-administered but seem quite effective. Later, it was discovered that the amino acids outside of and between the cysteines could be optimized, yielding the currently preferred sequence -FLNCCPGCCMEP-.<sup>32</sup> Advantages of the tetracysteine-biarsenical system include the very small size of targeting sequence, here 12 aa, and the abilities to detect newly synthesized peptide chains rapidly (< 1 min),<sup>33,34</sup> to measure the age of proteins by pulse-chase labeling with two different dyes on a time scale of hours to

days,<sup>35,36</sup> to correlate their fluorescence with electron microscopy,<sup>35,37</sup> to inactivate the protein's function in seconds to minutes,<sup>38</sup> and to monitor protein unfolding in situ.<sup>39</sup>

Subsequent approaches have been analogously introduced to label hexahistidine motifs with Ni<sup>2+</sup> or Zn<sup>2+</sup> complexes,<sup>40-42</sup> to enzymatically attach biotin or lipoic acid analogs to short acceptor peptides,<sup>43-45</sup> or to enzymatically replace a C-terminal -LPXTG motif by any tag with three glycines (GGG-) at its N-terminus.<sup>46</sup> Also, several full-sized protein domains can bind small molecules with sufficient specificity for in situ labeling, though in such cases there is no major size advantage over FPs. Three examples include the following: (1) *O*-alkylguanine transferase or a mutant reacts irreversibly with fluorescent benzyl derivatives of guanine or cytosine, respectively;<sup>47</sup> (2) antibodies raised against dyes as haptens can then bind those dyes and enhance their fluorescence;<sup>48</sup> and (3) a phytochrome protein from cyanobacteria has been mutated so that binding of its linear tetrapyrrole cofactor, phycocyanobilin, produces a brightly fluorescent holoprotein instead of the native nonfluorescent light-triggered histidine kinase. The long wavelength excitation and emission maxima (648 and 672 nm, respectively) and respectable extinction coefficient (measure of how strongly a molecule absorbs light, in this case 73,000 M<sup>-1</sup>cm<sup>-1</sup>) and quantum yield (probability that an excited molecule will reemit a photon, in this case > 0.1) could be of considerable interest for in vivo imaging.<sup>49,50</sup> In bacteria and plants, the phycocyanobilin can be added from outside or biosynthesized from heme via enzymes that have been cloned. Unfortunately, there are no publications showing this system works in animal cells, and preliminary experiments with exogenous phycocyanobilin or transfection of the biosynthetic enzyme have not been promising (X. Shu and R.Y. Tsien, unpublished).

### Sequestration of Critical Lone Pair of Electrons

The most common mechanism by which inorganic cations can directly affect the absorbance and fluorescence of synthetic small-molecule indicators is by electrostatically sequestering a lone pair of electrons on an oxygen or nitrogen atom within the chromophore.<sup>51,52</sup> Examples are shown in Figure 3. In each case, cation binding shifts the absorbance and excitation spectra to shorter wavelengths. When the cation binds to an aniline surrounded by additional coordination sites, the electrostatic sequestration is

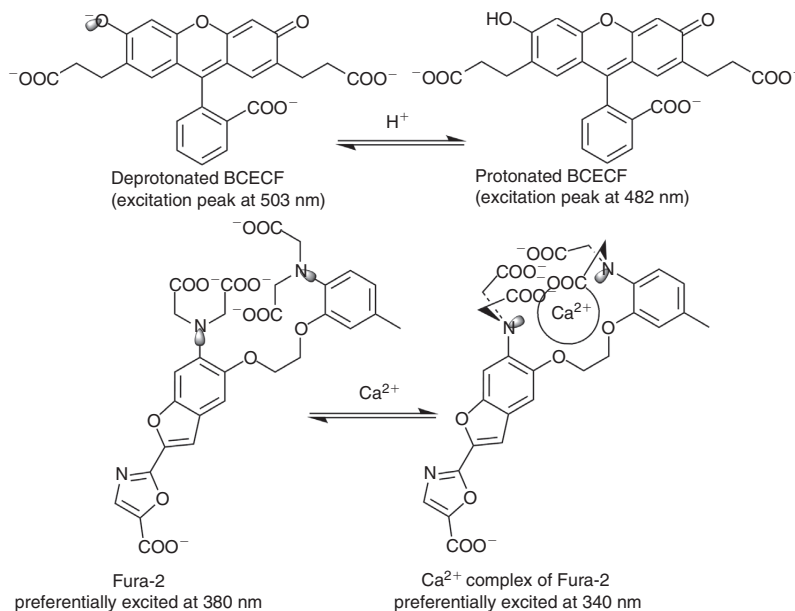


**Figure 3.** Structures of popular, representative small molecule indicators for which cation binding sequesters a crucial lone pair of electrons. The key lone pairs are indicated by electron clouds protruding from the relevant oxygen or nitrogen atoms. Top: the pH indicator BCECF. Bottom: the Ca<sup>2+</sup> indicator fura-2.

supplemented by twisting of the nitrogen-to-aryl bond, further disconnecting the lone pair from the rest of the chromophore. The most popular long-wavelength metal indicators, such as fluo-3, fluo-4, Calcium Green, Oregon-Green-BAPTA, and their analogs for other cations, only increase their fluorescence intensity upon metal binding, with very little or no wavelength shift. Here, the metal binding site is remote from yet connected to the actual chromophore. Excitation of the chromophore consists of promoting an electron from the highest occupied molecular orbital (HOMO) to the lowest unoccupied molecular orbital (LUMO). If the aniline is cation-free, it is electron-rich enough to donate an electron to fill the vacancy in the HOMO, thus stranding the electron in the LUMO and quenching fluorescence. If the aniline is cation-bound, it is no longer electron-rich enough to donate to the HOMO, so fluorescence is restored.<sup>51,52</sup> Although such indicators are the easiest way to get absorbance and emission maxima > 500 nm, their signals are hard (but not impossible<sup>53</sup>) to calibrate because changes in analyte concentration are hard to distinguish from changes in amount of dye, motion artifacts, fluctuations in excitation intensity, etc. In principle, excited state lifetime measurements could overcome this ambiguity by resolving metal-free from metal-bound indicator molecules.<sup>54</sup> Unfortunately, the

metal-free species is often undetectable because its emission is too weak and short-lived.

In some older metallochromic indicators, such as calcein or arsenazo III, the crucial phenols are surrounded by additional coordination sites to which the metal primarily binds, then forcing the phenol to deprotonate. Because the metal is further away from and less tightly bound to the phenolate oxygen than the proton had been, the metal shifts the spectrum from that of the neutral phenol toward that of the phenolate anion. These indicators have the severe disadvantage that their metal responsiveness is limited to a narrow range of pH because of two intrinsic pH-sensitivities. At low pH, the metal has increasing difficulty displacing the proton, whereas at high pH, the phenol has already lost its proton, so metal binding has little spectral effect.

### Modulating of Quenching by Dye Aggregation

Another important way to quench fluorophores is simply to pack them together at high effective concentrations, typically in the millimolar range. One explanation is that identical fluorophores often like to stack side-by-side with their flat faces in contact to minimize hydrophobic

interactions with water. Any excitation of the dimer immediately relaxes to a lower-energy composite quantum state in which the excitation is spread between both fluorophores but whose transition dipoles are anti-parallel. This state is nonfluorescent because destructive interference between the oppositely-oriented transition dipoles hinders photon emission during any attempt to return to the ground state.<sup>55</sup> Many other explanations have also been proposed.<sup>56</sup>

Whatever the quantum mechanical explanation, quenching by crowding has been empirically useful as a way of sensing any biochemical process that allows packed fluorophores to disperse and escape quenching. Thus, if membrane-impermeant fluorescent dyes are loaded at high concentration inside vesicles, leakage of those vesicles or fusion with unloaded vesicles dilutes the dye molecules and increases fluorescence per molecule. Dyes attached at high density to a vesicular membrane likewise dequench when that membrane fuses with unlabeled membranes, permitting dilution by lateral diffusion.<sup>57</sup> Dyes closely packed on polymers or proteins dequench when the polymers or proteins are disassembled, proteolyzed, or even unfolded by applied tension.<sup>56</sup> This effect has become a very popular method for visualizing local proteolysis, both in culture and in live animals.<sup>58–61</sup> Another variation is to image lysosomal proteolysis after ligand endocytosis.<sup>62</sup> However, one fundamental ambiguity should be kept in mind when imaging local dequenching by disassembly or proteolysis: the fluorescence increase should not be sustained but should reverse as fluorophores diffuse away from their site of release.

### Single FP: Perturbation of Chromophore Protonation

As shown in Figure 2, most emission from FPs stems from deprotonated chromophores, so any biochemical signal that affects the degree of deprotonation will affect fluorescence. The most obvious signal is pH. The earliest discovered FP, *Aequorea* Green FP, contains about 6:1 protonated:deprotonated chromophores in its wild-type ground state,<sup>63</sup> explaining why the excitation spectrum has a major peak at ~395 nm and only a minor peak at 475 nm. This ratio is surprisingly indifferent to external pH between 4 and 11, implying that the fluorophore is well insulated from external protons until extreme pH's begin to denature the protective  $\beta$ -barrel.<sup>64</sup> However, absorption of a photon strongly favors deprotonation of the fluorophore, so that both excitation peaks give a common emission peak at 510 nm.<sup>65</sup> The

ground state protonation ratio at pH 7 can be forced to full protonation (excitation only near 400 nm) versus deprotonation (excitation only at 475 nm, with much greater amplitude) by different mutations, for example, T203I versus S65T, respectively.<sup>9,66</sup> For most purposes, it is preferable to put the maximum amplitude into the longer-wavelength excitation peak, so most routine applications of GFP as a passive tracer now incorporate S65T or equivalent mutations. However, S65T will reversibly protonate with a  $pK_a$  of 6.15, and other mutants give both higher and lower  $pK_a$ 's, so appropriate FPs genetically targeted to different subcellular locations are amongst the best ways to measure pH in those compartments.<sup>67</sup> Most secretory granules are quite acidic internally, pH ~5, so exocytosis can be monitored as pH-sensitive FPs targeted to the vesicle lumen go from such acidic pH to pH 7.4 in the extracellular medium.<sup>68</sup>

In other mutants of GFP, the protonation state of the chromophore has been accidentally or deliberately engineered to respond to a variety of signals other than pH, including halide ion concentrations,<sup>69</sup> thiol-disulfide redox potentials,<sup>70,71</sup> hydrogen peroxide,<sup>72</sup> singlet oxygen,  $Ca^{2+}$  ions,<sup>73–78</sup> and even membrane potential.<sup>79</sup> It is often helpful to do circular permutation of the FP, that is, connect the original N- and C-termini by a peptide linker and generate new N- and C-termini at a new location on the  $\beta$ -barrel (Figure 4). The resulting permutants generally seem a little more conformationally flexible than FPs with wild-type topology, making it easier for other protein domains fused to the new N- or C-termini to affect the protonation state of the internal fluorophore.<sup>73</sup> A generic caution for all these sensors based on chromophore protonation is that they are still somewhat or very sensitive to pH over certain ranges.

### FRET

FRET is a quantum-mechanical interaction between a donor fluorophore and an acceptor chromophore that can absorb some of the wavelengths at which the fluorophore would normally emit.<sup>6,80</sup> The acceptor chromophore may be, but does not have to be fluorescent. If the fluorophore and chromophore are within a few nanometers of each other and are appropriately oriented with respect to each other, then the excited state of the donor fluorophore can directly transfer its energy to the acceptor chromophore without emission and reabsorption of a photon. The resulting excited acceptor behaves just as if it had gotten its energy from a real photon, so if it is fluorescent, it can reemit at yet longer wavelengths.

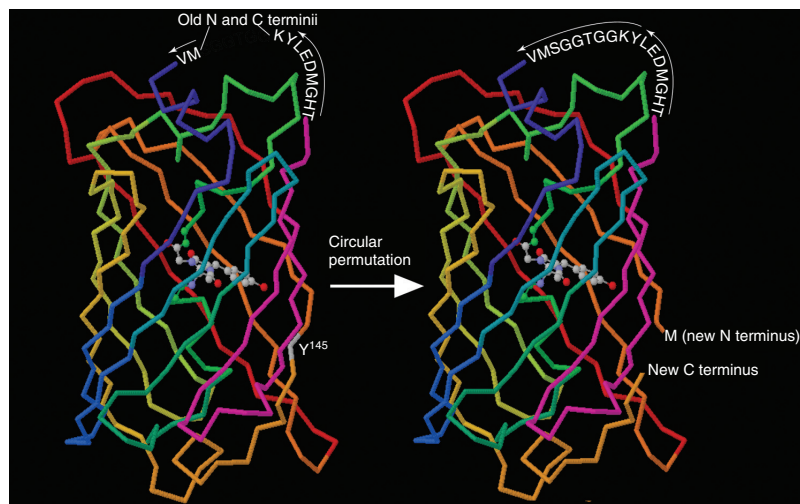


**Figure 4.** Schematic showing how circular permutation rearranges the topology of a fluorescent protein, such as GFP. Left:  $\alpha$ -carbon backbone and chromophore of GFP before permutation. Colors of the  $\alpha$ -carbon backbone range from blue at the N-terminus through the visible spectrum to magenta at the C-terminus simply to help the eye trace the sequence of strands. Amino acids MV at the N-terminus and THGMDELYK at the C-terminus are written as text because they are too disordered to have coordinates in the crystal structure. Right: GFP circularly permuted with new N- and C-termini created at Tyr-145 and the former N- and C-termini connected with a GGTGGS linker. See Baird GS *et al.*<sup>73</sup> for further details on the construction and properties of this circular permutant.

Because FRET depends strongly on donor-acceptor distance and orientation, it can be a sensitive readout of association equilibria and conformational changes.<sup>81</sup> In intact cells and organisms, the donor and acceptor are nowadays almost always FPs or genetically targeted small molecules, so that they can be precisely attached to the host protein(s) and so that the resulting chimera can be targeted to the appropriate location(s).

FRET can be monitored by many different spectroscopic techniques.<sup>82</sup> The most common is to use a fluorescent acceptor and monitor the ratio of emissions at wavelengths characteristic of the acceptor and the donor, respectively. This ratio increases as FRET increases, but quantitative calibration of this emission ratio in terms of FRET efficiency requires mathematical corrections for the extent to which the donor emits within the acceptor's emission band, the extent to which the donor excitation wavelength also directly excites the acceptor and the quantum yields of the isolated donor and acceptor.<sup>83–85</sup> A mathematically simpler procedure is to observe how much the donor gets brighter when the acceptor is selectively photobleached, but this calibration is destructive, relatively slow, and requires that the amount of donor in each pixel remain unchanged during such destruction of the acceptor.<sup>86</sup> FRET can be elegantly and nondestructively quantified by its diminution of the excited state

lifetime of the donor,<sup>87</sup> but the instrumentation to make such measurements is expensive and rare, and the signal acquisition times are much longer than for collection of emission ratios. Finally, FRET can occur to some extent between identical fluorophores due to the modest overlap between excitation and emission spectra. Such “homo-FRET” is particularly useful for assessing homodimerization but can only be detected by a reduction in the polarization of the emission.<sup>88</sup>

The fundamental advantages of FRET are its generality, well-defined quantitative basis, sensitivity to small changes in distance or orientation, instantaneous kinetics (within the nanosecond excited state lifetime), and complete reversibility. Also, FRET does not require that donor and acceptor touch each other, and it does not introduce any extra attraction or repulsion between them. On the other hand, FRET becomes very weak beyond 6 to 8 nm, which is too short a range for many interacting protein complexes. Even within that distance range, FRET usually causes quite subtle changes in the composite emission spectrum, far from an all-or-nothing signal, so careful quantitation is required. One almost never knows the relative orientation of the donor and acceptor fluorophores, and the traditional simplifying assumption of random orientation is unreliable for fluorophores as large as FPs,<sup>89</sup> so orientation becomes a significant unknown perturbant.

A useful relative of FRET is bioluminescence resonance energy transfer (BRET), in which the donor is a bioluminescent protein.<sup>90-92</sup> Generation of the excited state by chemical decomposition rather than photon absorption makes no difference to the subsequent interaction with a neighboring acceptor. BRET shares the above features of FRET and furthermore avoids the problems of autofluorescence background and difficult penetration of excitation light. On the other hand, BRET shares the generic weaknesses of bioluminescence, such as requirement for cofactors, low light output per molecule, and inability to apply tricks based on excitation control, such as excited state lifetime measurements, polarization measurements, and multiple excitation locations and beam directions to aid tomographic reconstruction.

## Other Proximity Assays

### FP Complementation

Many proteins can be expressed as two separate fragments that if held in close proximity can refold together and reconstitute the function of the native protein.<sup>93,94</sup> FPs might seem too particularly hard to reconstitute from separate fragments because the  $\beta$ -barrel looks so monolithic. However, the tolerance of FPs to circular permutation<sup>73</sup> suggested that fragment complementation might work, which proved to be true. Thus, co-expression of residues (1 to  $x$ ) of GFP fused to protein X, plus residues ( $x$  to 238) of GFP fused to protein Y, where  $x = 155$  or  $173$ , generates fluorescence only if X and Y form a complex.<sup>95-97</sup> A further extension is to mix and match fragments derived from cyan fluorescent protein (CFP) and yellow fluorescent protein (YFP); the resulting hybrid proteins show spectra intermediate between those of their parents.<sup>98</sup> By contrast, fragments consisting of amino acids 1 to 214 and 215 to 230 of a superfolder GFP, each individually nonfluorescent, spontaneously reassociate to give fluorescence without requiring any partners to splint them together.<sup>99</sup> Presumably these fragments have a much higher association constant than those split at 155 or 173, but these association parameters have not been measured. The great advantage of such complementation methods (also applicable to bioluminescent proteins and many enzymes<sup>93,94</sup>) is their all-or-nothing response, so that it is easy to qualitatively detect low levels of interaction. On the other hand, there is little or no quantification of how strong or stable the interaction between X and Y must have been to generate the observed signal. False negative results could result if the X-Y complex does not put the FP fragments into the correct orientation and close proximity, but this possibility

has not yet been documented. Folding and reconstitution of intact function is slow and irreversible for FPs.

### Activatable Cell-Penetrating Peptides

Another type of proximity assay is based on cell-penetrating peptides<sup>100</sup> (CPPs, also known as protein transduction domains or PTDs), which are polycationic peptides or oligomers that strongly adhere to the negatively charged surfaces (particularly proteoglycans) of cells and are then internalized, mostly by endocytosis. Payloads, such as imaging or therapeutic moieties, attached to the CPPs are thus taken up into cells, though much or most may remain trapped inside organelles. A polyanionic peptide fused to the CPP through a linker vetoes uptake, probably by forming a hairpin with the polycation and neutralizing the latter's positive charge. Cleavage of the linker, for example, by proteolysis, releases the polyanion, removes the inhibitory constraint, and frees the CPP. Thus, such activatable cell-penetrating peptides (ACPPs) localize CPP-mediated retention and uptake of payloads in the immediate vicinity of extracellular proteases or other activities (eg, reduction of a disulfide) that can cut whatever linker connects the polyanion to the polycation.<sup>101-103</sup> This mechanism is functionally somewhat analogous to FRET because the polycation and polyanion are analogous to donor and acceptor, respectively, and proximity quenches cell uptake rather than fluorescence. In some ways ACPPs are the inverse of FP complementation, in that the interaction of the two peptide segments is antagonistic rather than synergistic, so the assay detects dissociation rather than association. The biggest advantage is that the payload does not have to be fluorescent but can be species as diverse as magnetic resonance imaging contrast agents or bacteriophages.<sup>104,105</sup> The only known limitation on the payload is that it must not mask and neutralize the polycation. Thus, naked oligonucleotides are probably poor payloads because of their multiple negative charges.

## PATHWAYS COMMONLY MONITORED BY FLUORESCENCE

### Transcription and Translation<sup>106</sup>

#### Reporter FPs

The earliest<sup>107</sup> and probably still most common applications of FPs are as transcriptionally controlled reporter genes.<sup>108</sup> Fluorescence can thus monitor which cells have



been transfected, which cells express a tissue-specific promoter, which promoter regions are activated, etc. Typically, the FP is left unfused, but recently the highest sensitivity has been obtained by fusing a bright YFP to a membrane protein and thus restricting Brownian motion.<sup>109</sup> Transcriptional generation and translation of a single messenger RNA (mRNA) molecule generated bursts of fluorescence in an *Escherichia coli* cell as the reporter YFP fusions matured their chromophores then bleached in the intense laser excitation. In this regime, the temporal fidelity with which translation can be reported is limited by the maturation time of the FP. Proteolytic degradation of the FP is irrelevant because photobleaching is much quicker. However, most uses of FPs to report transcription and translation are done with large populations of molecules per cell observed at much lower excitation intensities. Under these conditions, the intrinsic maturation time of the FP may not be limiting if it takes much longer simply to build up enough FP to be seen over background. Also the fluorescence as a function of time is governed not just by protein synthesis but also by degradation. FPs themselves are relatively long-lived and resistant to proteolysis. The instantaneous fluorescence more faithfully reflects the rate of translation if the FP is destabilized by appending degradation-promoting sequences,<sup>110,111</sup> though the inevitable trade-off is a decrease in sensitivity. This trade-off should be avoidable if the biological system and instrumentation allow higher excitation intensities so that the FP can be simultaneously read out and destroyed by photobleaching or photoconversion to a different color.

For tracking the fates of multiple cells in the same organism, the sizable number of distinctly colored individual FPs can be combinatorially multiplied by targeting to different subcellular locations as well as ingenious permutations of genetic recombinations controlled by the Cre/lox system. More than a hundred color combinations can be distinguished.<sup>112,114</sup>

When the focus is on the rate of translation in isolation from transcription, variations in transcription or mRNA stability can be corrected for if the same vector additionally encodes an FP of a different color, ideally under the control of an internal ribosome entry sequence (IRES).<sup>114–116</sup> The ratio of signals from the test and reference FPs isolates translational modulation of the former.

The above readouts focus on the rates of transcription and translation. For investigations on the subcellular locations of these processes, the relevant DNAs or mRNAs can be indirectly visualized by inclusion of multiple tandem repeats of polynucleotide sequences (eg, lac operons for DNA<sup>117,119</sup> or MS2<sup>118,119</sup> for mRNA) for which high-affinity specific binding proteins (eg, lacI or

MS2-binding protein) are known. Co-expression of those binding proteins fused to FPs of different colors causes fluorescent dots to appear at the relevant loci of the DNA or mRNA. Such techniques have limitations, such as the large bulk and potential perturbations introduced by the multiple nucleic acid repeats and binding protein-FP fusions. But with appropriate controls, they have yielded much biological insight. Likewise, selected protein constituents of transcription complexes or ribosomes can be fused to FPs for intact cell localization or in vitro biophysical measurements.<sup>120</sup>

### Reporter Enzymes with Fluorogenic Substrates<sup>106,121</sup>

An additional amplification stage can be incorporated if the reporter protein is not an FP but rather an enzyme that rapidly converts nonfluorescent substrates into fluorescent products or changes the color of the substrate. The costs of this increased sensitivity are the need to synthesize and administer the substrate and the loss in spatial and temporal resolution. Many such fluorogenic reporter enzymes have been introduced, including alkaline phosphatase,<sup>122</sup>  $\beta$ -galactosidase (the product of the *lacZ* gene),<sup>123</sup> RTEM  $\beta$ -lactamase (the product of the ampicillin-resistance gene),<sup>124</sup> and uroporphyrinogen III-methyltransferase (the product of the *cobA* gene).<sup>125</sup> The first two enzymes generate fluorescence by cleaving phosphate and galactose respectively off phenolic groups within dyes. Because phosphates and galactosides are much more hydrophilic than free phenols, the enzyme substrates are much less membrane-permeant than the products. Therefore, it is difficult both to get the nonfluorescent substrates into living cells and to retain the fluorescent products there. Therefore, it may be better to put the reporter enzyme on the outside of cells, where impermeant substrates have relatively free access, then trap the fluorescent product either by precipitation<sup>122</sup> or acetoxymethyl (AM) ester hydrolysis.<sup>123</sup>  $\beta$ -lactamase substrates are more inherently suitable for imaging of single live cells because enzyme expressed in the cytosol attacks the  $\beta$ -lactam linker, splitting two dye molecules apart, disrupting FRET, and increasing the net charge on the products. The loss of FRET gives a very large increase in blue/green emission ratio, enabling quantitative and very sensitive measurements on fully viable single cells, especially by flow cytometry.<sup>124,126,127</sup> The unique advantages of uroporphyrinogen III-methyltransferase is that its substrate is the ubiquitous intermediate in heme biosynthesis, uroporphyrinogen III, and that its product (sirohydrochlorin) is red fluorescent. Despite its unique ability to generate long-wavelength fluorescence without an

exogenous substrate, this reporter enzyme<sup>125</sup> has been surprisingly little-used.

### Protein Trafficking and Degradation

Nowadays, the dominant way to image protein trafficking and degradation is to fuse the protein of interest to an FP, preferably one engineered to delete any tendency to oligomerize.<sup>13,21</sup> In principle, the FP can be genetically appended to either end of the host protein. If both termini of the host protein are sacrosanct, then the FP can often be inserted within the host protein sequence, typically at an internal loop. Assuming a fusion can eventually be found that has a similar function and fate as the untagged protein, and that the FP is not split off before the entire chimera is eventually degraded, imaging shows directly the spatial distribution of the protein of interest at or approaching steady state.

The fate of the protein can be probed with greater spatiotemporal resolution by choosing FPs whose fluorescence properties can be locally or kinetically varied.<sup>128</sup> The simplest case are “fluorescent timers,” FPs whose color gradually changes from green to red due to intrinsically slow kinetics of maturation, so that the average age of the FP or fusion can be judged by the color.<sup>129,130</sup> Unfortunately, existing fluorescent timers are still obligate tetramers. Also, the time resolution is limited by the gradual nature of the color change at the population level or the stochastic variation in maturation time at the single molecule level. Better time resolution is obtainable with an external stimulus. Some early FPs, including wild-type *Aequorea* GFP, refused to become fluorescent if expressed above a permissive temperature, so one could selectively image those copies synthesized during a period of lower temperature.<sup>131</sup> Because temperature steps have so many nonspecific biological effects, such modulation was soon superseded by photochemical triggering, that is, use of actinic light to switch fluorescence on or off or to change its color. Such modulation can now be either reversible or irreversible depending on the exact FP and conditions of irradiation. Because light can be localized with great precision, local photochemical triggering also enables monitoring of the movement of fusions between spatial compartments. For further information on this complex topic, the reader is referred to recent reviews.<sup>128,132–134</sup>

Permeant small molecules can also be used to trigger the recording of the age and turnover of proteins. One approach is via the genetically encoded tags discussed in section “Genetically Targeted Small Molecules.” Assuming the incorporation of the small-molecule fluorophore into

the peptide tag is saturating and irreversible, administration of one species of small molecule labels all the fusion proteins made up to that point. If excess unbound dye is washed out, then a fluorophore of a different color is administered, it labels only the newer copies of protein, that is, those synthesized after washout of the first dye.<sup>35,36,47</sup> Although small molecules cannot be delivered and removed as precisely as photons can, appropriate small-molecule tags permit imaging by nonoptical modalities, such as electron microscopy,<sup>35,37</sup> and tracking of posttranslational modifications, such as glycosylation.<sup>135</sup>

A different form of pharmacological triggering has more potential to work in intact animals. Here, the protein of interest is genetically fused via a cis-acting protease to any easy-to-detect label, such as an epitope tag or FP. Once the polypeptide emerges from the ribosome, the constitutively active cis-acting protease cleaves itself from both its flanking partners, leaving the protein of interest untagged and unperturbed. But once a small-molecule inhibitor of the protease is administered, cleavage stops, so all newer copies of the protein of interest remain tagged and can be imaged by retrospective histology.<sup>136</sup> Currently, the preferred cis-acting protease is that of hepatitis C virus because this protease is monomeric, structurally and biochemically well characterized, quite specific in its substrate preferences, and inhibited by membrane-permeant drugs already developed by the pharmaceutical industry.

### Exocytosis and Endocytosis<sup>137</sup>

Techniques for monitoring rapid exocytosis and endocytosis have been the focus of special attention because of the importance of these trafficking events in synaptic transmission and endocrine secretion. Small amphiphilic styryl dyes with two permanent positive charges, such as FM1-43 and FM4-64, intercalate tightly to the outer leaflet of the plasma membrane but do not flip-flop across it. Membrane-bound dye is highly fluorescent, whereas aqueous dye is practically nonfluorescent. Thus, exocytosis can be monitored either by the increase in fluorescence as previously unstained vesicular membrane is added to the plasma membrane and becomes exposed to free dye or by the subsequent washout of fluorescence as previously stained and endocytosed vesicular membrane is once again exocytosed into dye-free medium.<sup>138</sup> More recently, pH-sensitive FPs have provided a genetically encoded alternative.<sup>139</sup> If an appropriate FP is fused to the luminal face of a vesicular membrane protein, its fluorescence is quenched by acidic pH (~5) in the lumen, switched on by normal extracellular pH (~7.4) upon

exocytosis, then quenched gradually upon endocytic recycling and reacidification. This fluorescence readout can be used either to study synaptic biology or to monitor *in vivo* neuronal activity.<sup>137,140</sup>

### RNA Trafficking

Unfortunately, no direct equivalent of FPs is known for RNA, that is, a nucleotide sequence that folds up and spontaneously generates an internal fluorophore. In analogy to the peptide tags of section “Genetically Targeted Small Molecules,” RNA aptamers are known that bind membrane-permeant nonfluorescent dyes, such as Malachite Green with submicromolar dissociation constants and enhance the dye fluorescence several 1000-fold, attaining respectable quantum yields.<sup>141</sup> Unfortunately, the same dyes also become fluorescent upon nonspecific binding to other intracellular constituents, so these aptamers have not yet enabled imaging of RNAs within live cells. Distant membrane-permeant analogs of Malachite Green do not show significant fluorescence upon contact with mammalian cells (S.R. Adams, J. Babendure, and R.Y. Tsien, unpublished data), so the powerful techniques of *in vitro* RNA evolution should be able to generate tight-binding, fluorescence-enhancing aptamers against these more suitable dyes. Meanwhile, the main approach currently available is to fuse the RNA of interest to multiple copies of a 19-nucleotide stem-loop sequence that binds specifically and tightly to a dimeric coat protein from bacteriophage MS2. This MS2 protein is co-expressed as a fusion to an FP, which therefore lights up the RNA of interest.<sup>119</sup> Once multiple copies of the stem-loop have attracted equal numbers of MS2-FP fusions, many hundreds of kilodaltons have been added to the RNA of interest, but much biology has been learned nevertheless. To reduce background fluorescence, excess copies of MS2-FP fusion should be avoided, or two RNA sequences each binding a different protein should be juxtaposed. In turn, the two RNA-binding proteins are fused to complementary fragments of a split FP, so that fluorescence only develops after the two RNA-binding proteins find each other on the same piece of RNA.<sup>142</sup>

### Inorganic Ion Concentrations

#### H<sup>+</sup>

Cytosolic pH can be measured with a range of small-molecule fluorescent probes, perhaps the most popular of which is a fluorescein derivative, BCECF, designed to

have an optimized pK<sub>a</sub>, improved cellular retention, and excitation ratiometric readout.<sup>143</sup> The obvious genetically encoded alternatives are pH-sensitive FPs, which are especially advantageous if targeting to specific organelles or subcellular locations is desired. Most FPs become brighter overall as the pH increases, until extreme alkalinity causes irreversible denaturation. The pK<sub>a</sub>'s cover a wide range; alkaline pK<sub>a</sub>'s are most readily available from circularly permuted FPs.<sup>73</sup> A few FPs have been evolved to have ratiometric readouts, that is, pH-dependent changes in peak excitation or emission wavelength.<sup>144,145</sup>

#### Ca<sup>2+</sup>

Techniques for measurement and imaging of intracellular Ca<sup>2+</sup> have undergone intensive development due to the ubiquitous biological importance of this ion in cell signaling. In addition, Ca<sup>2+</sup> signals are often the most convenient readout for cell activation in neuronal networks<sup>146</sup> and pharmaceutical drug screening. The chemical challenge in sensing intracellular Ca<sup>2+</sup> is that the relevant range of free concentrations is 10<sup>-8</sup> to 10<sup>-7</sup> M in quiescent cells, rising to 10<sup>-6</sup> to 10<sup>-5</sup> M in activated cells, sometimes for only a few milliseconds. Meanwhile, both intracellular Mg<sup>2+</sup> and extracellular Ca<sup>2+</sup> are roughly 10<sup>-3</sup> M, so the indicator must have at least five orders of magnitude selectivity for Ca<sup>2+</sup> over Mg<sup>2+</sup>, and it must be introduceable into the cytoplasm without causing any significant leakage in the plasma membrane. The organic chemical solutions<sup>51,143</sup> to these challenges are mostly derivatives of BAPTA, 1,2-bis(2-aminophenoxy)ethane-*N,N,N',N'*-tetraacetic acid, whose metal-binding site fits well-around Ca<sup>2+</sup> but is too large for Mg<sup>2+</sup> to fit snugly. Ca<sup>2+</sup> alters the spectra by sequestering the lone-pair electrons on nitrogen (see section “Sequestration of Critical Lone Pair of Electrons”). Ca<sup>2+</sup> affinities and spectral properties, including excitation/emission wavelengths from UV to near-infrared (IR), are tuned by the choice of substituents on the two aromatic rings of BAPTA. These polycarboxylic acids can be esterified with AM groups to generate uncharged, lipophilic derivatives, which can diffuse across the plasma membrane. The esters are then hydrolyzed by intracellular esterases to regenerate the polyanions, which are thus trapped inside the cell, mostly in the cytoplasm, though under some circumstances accumulation in organelles can also occur. Though the by-products of AM ester hydrolysis are acetic acid and formaldehyde, these are generated slowly enough and at low enough concentration not to cause noticeable toxicity except in especially sensitive tissues, such as retina, which require coadministration of formaldehyde antidotes.<sup>51,147</sup> AM esters can even load

large numbers of neurons within intact brain to permit imaging of firing patterns in neuronal networks.<sup>148,149</sup> Higher loadings can buffer  $\text{Ca}^{2+}$  during excitotoxicity.<sup>150</sup>

A greater number of genetically encoded indicators have been created for  $\text{Ca}^{2+}$  than for any other analyte.<sup>148,151</sup> Most are based on the endogenous  $\text{Ca}^{2+}$  sensor calmodulin (CaM), which binds four  $\text{Ca}^{2+}$  then wraps itself around a target peptide, of which the most commonly chosen is M13, derived from skeletal muscle myosin light chain kinase.  $\text{Ca}^{2+}$  affinities can be tuned by mutation of the binding sites within CaM, for example, by changing glutamates to glutamines. Cross-reactivity with ubiquitous endogenous CaM or CaM-binding domains can be reduced by introducing compensating mutations into both CaM and M13<sup>152</sup> or by switching the  $\text{Ca}^{2+}$  sensor to troponin C,<sup>153</sup> which is endogenously abundant only in skeletal muscle. The final mechanism for fluorescence responsiveness can be modulation either of the protonation state of a single FP<sup>73–78</sup> (see section “Single FP: Perturbation of Chromophore Protonation”) or the mutual orientation and FRET efficiency between a donor FP and an acceptor FP (see section “FRET”).<sup>89</sup> Although the genetically encoded indicators give far greater precision of localization anywhere within the transfected cell or organism and are self-renewing, they still give much smaller fractional changes in fluorescence intensity or ratio and slower reaction kinetics than their small-molecule counterparts.<sup>146</sup> For the specialized challenge of measurement of fast  $\text{Ca}^{2+}$  transients in nanodomains, such as within nanometers of the mouth of  $\text{Ca}^{2+}$  channels, a hybrid solution is possible: small-molecule  $\text{Ca}^{2+}$  indicators with biarsenical substituents, which localize to tetracysteine motifs (see section “Genetically Targeted Small Molecules”) genetically placed within the channel sequence.<sup>154</sup>

#### Miscellaneous Metal Cations

BAPTA and its derivatives also bind many other divalent and trivalent cations, for example,  $\text{Sr}^{2+}$ ,  $\text{Ba}^{2+}$ ,  $\text{Mn}^{2+}$ ,  $\text{Zn}^{2+}$ ,  $\text{Cd}^{2+}$ ,  $\text{Pb}^{2+}$ , and lanthanides.<sup>51</sup> Fortunately, these ions are normally at negligible free concentrations in cells, allowing the dyes to measure  $\text{Ca}^{2+}$ . In some tumor cell types<sup>155</sup> or when normal cells are challenged with unusual levels of heavy metals,<sup>156–159</sup> signals from heavy metals become significant and can be disentangled from  $\text{Ca}^{2+}$  signals if sufficient care is taken. Selectivities can be shifted toward first row “hard” transition metals by replacing carboxylates by pyridine ligands.<sup>160</sup> To sense monovalent cations, the

multiple carboxylate anions are replaced by neutral macrocyclic rings, for example, diazacrown ethers.  $\text{Na}^+$  favors 15-membered, pentacoordinating rings, whereas  $\text{K}^+$  prefers 18-membered, hexacoordinating rings.<sup>161</sup> Protein-based indicators for  $\text{Zn}^{2+}$  have been based on Zn-fingers,<sup>17</sup> metallothionein,<sup>162</sup> carbonic anhydrase,<sup>163</sup> and *de novo* cysteines and histidines causing FP dimerization.<sup>164</sup> FRET sensors for  $\text{Cu}^+$  and  $\text{Zn}^{2+}$  can be engineered from copper chaperones.<sup>165</sup> Unfortunately, few if any protein domains have been characterized that undergo large conformational changes selectively in response to metal ions other than  $\text{Ca}^{2+}$ ,  $\text{Cu}^+$ , and  $\text{Zn}^{2+}$ . When such domains are isolated, it should be possible to incorporate them into genetically encoded sensors by perturbation of FP chromophore protonation or by FRET.

#### $\text{Cl}^-$ and Orthophosphate

A few fluorescent dyes containing quaternized heterocyclic cations are quenched by encounter with  $\text{Cl}^-$ , permitting their use as chloride indicators.<sup>166,167</sup> They are somewhat difficult to use because of short wavelengths, easy bleaching, and poor trappability inside cells. Genetically encoded indicators became possible with the discovery that some but not all YFPs have a cavity near the chromophore into which halide ions can fit.<sup>69</sup> The bound anion electrostatically promotes protonation of the chromophore, which diminishes fluorescence, an example of the mechanism discussed in section “Single FP: Perturbation of Chromophore Protonation.” This quenching can be converted into a ratiometric readout by fusion of a pH-insensitive CFP to the halide- and pH-sensitive YFP.<sup>168,169</sup>  $\text{Cl}^-$  binding decreases both the spectral overlap of YFP excitation with CFP emission, which FRET requires, as well as the quantum yield for YFP reemission.

Orthophosphate ( $\text{H}_2\text{PO}_4^-$  and  $\text{HPO}_4^{2-}$ ) can be sensed by fusing a bacterial phosphate-binding protein between CFP and YFP and monitoring the change in FRET from the CFP to YFP moieties.<sup>170</sup>

#### Small Organic Molecules

##### Amino Acids and Sugars

Fluorescent indicators for a variety of important small organic molecules including amino acids (eg, glutamate and tryptophan) and sugars have been created by the same strategy, that is, insertion of a periplasmic analyte-binding protein between CFP and YFP.<sup>171</sup> Glutamate

has received the most biological attention because of its importance as the major excitatory neurotransmitter in the mammalian CNS.<sup>172,173</sup> The original *E. coli* glutamate binding protein GltI has too high an affinity to sense the peak concentrations around mammalian synapses, but it is relatively easy to reduce affinities mutagenically. Optimization of the FRET response required systematic searching of sequence space, truncation of 0 to 15 amino acids from the N-terminus, and 0 to 10 amino acids from the C-terminus of GltI ( $16 \times 11 = 176$  combinations). The fitness landscape, that is, plot of response versus number of amino acids truncated from the N- and C-termini, was surprisingly jagged, in that the best performer, with eight and five deletions from N- and C-termini, respectively, was surrounded on all sides by very poorly performing neighbors. This experience suggests that high-throughput generation and testing of systematic variations may be required to optimize FP-based FRET reporters.<sup>172</sup>

### Cyclic Nucleotides

Cyclic nucleotides, cyclic adenine monophosphate (cAMP) and cyclic guanine monophosphate (cGMP), are important second messengers that necessarily bind to and activate several endogenous sensor proteins during their signal transduction cascades. These natural transducers can be converted into fluorescent indicators.<sup>174</sup> The cAMP-induced dissociation of catalytic (C) and regulatory (R) subunits of protein kinase A can be monitored by loss of FRET between fluorescein and rhodamine labels on C and R, respectively.<sup>175</sup> This composite indicator produced important biological insights into cAMP signaling in invertebrate neurons.<sup>176,177</sup> However, the difficulties of attaching dyes to recombinant proteins *in vitro*, reconstitution of holoenzyme, and microinjection back into cells, were primary motivations for the original development of FPs with different colors suitable for FRET. After much trial and error, viable fusions of C and R to GFP and BFP and later to YFP and CFP were developed.<sup>178,179</sup> Such fusions made introduction into transfectable cells much easier, but left the problems of balancing the expression level of two separate gene products, and potential cross-reaction with endogenous unlabeled R and C subunits. Therefore, alternative FRET-based indicators for cAMP have been created from a cAMP-activated guanine nucleotide exchange factor, Epac.<sup>180–182</sup> Indicators for cGMP can likewise be engineered from cGMP-dependent protein kinase (PKG), either sandwiched between donor and acceptor FPs<sup>183,184</sup> or fused to a single circularly-permuted FP.<sup>185</sup> Both Epac and PKG

change conformation upon binding cAMP or cGMP respectively but do not dissociate into separate subunits as protein kinase A does. Cyclic nucleotide signaling can also be monitored at the next downstream mechanistic stage, the activation of endogenous protein kinase A or G (see section “Kinase and Phosphatase Activities”).

### Ins(1,4,5)P<sub>3</sub>

Several indicators for the Ca<sup>2+</sup>-mobilizing messenger Ins(1,4,5)P<sub>3</sub> have been based either on translocation of tagged pleckstrin homology domains from plasma membrane to the cytosol, or on FRET between FPs flanking portions of the Ins(1,4,5)P<sub>3</sub> receptor.<sup>186</sup>

### Guanosine Triphosphate/Guanosine Diphosphate Status of G Proteins

Because of the widespread importance of both heterotrimeric and small guanosine triphosphate (GTP)-binding proteins (G proteins) in signal transduction, much effort has been devoted to imaging their state of activation in live cells, that is, whether they are bound to GTP versus GDP. One direct strategy is to fuse an FP to the G protein of interest, for example, Ras, microinject GTP tagged with a small dye Bodipy-TR, and observe FRET from the FP to the dye, preferably at the level of single molecules so that colocalization of the two fluorophores and their diffusional trajectories can also be resolved.<sup>187</sup> One concern is that hydrolysis of the bound Bodipy-TR-GTP might occur and might not be spectroscopically obvious, in which case the observations might include inactive Ras. Another approach, which avoids microinjection and can be wholly genetically encoded, is to fuse an FP to a protein domain known to bind only to one form of the G protein.<sup>188,189</sup> For example, the Ras-binding domain from the effector protein Raf-1 binds Ras-GTP, not Ras-GDP. Such binding can be detected by intermolecular FRET, for example, from CFP-tagged Ras to YFP-tagged Ras-binding domain. Alternatively, the G protein, the effector domain, and the donor and acceptor FPs can be fused in various orders into four-part chimeras in which intramolecular FRET reflects activation status of the exogenous G protein.<sup>189,190</sup> Activation of endogenous unlabeled G proteins at particular subcellular locations, for example, plasma membrane versus Golgi, can be qualitatively imaged by translocation of FP-tagged binding domains from the cytosol to those sites.<sup>188</sup> Results with heterotrimeric G proteins have been more complex and controversial. Whereas the classical view is that  $\beta\gamma$  subunits bind to  $\alpha$ -guanosine diphosphate and

dissociate from  $\alpha$ -GTP, there is increasing evidence from FRET and BRET experiments that in some cases, activation causes only a conformational change, not overt dissociation.<sup>191</sup>

### Redox Potential; Reactive Oxygen, and Nitrogen Species

Most of the redox couples in cells are not in equilibrium with each other, which is fortunate because ultimate equilibrium with atmospheric  $O_2$  would require most biological molecules to burn up. Therefore, many separate redox potentials could be defined. Thiol-disulfide exchange is one of the few biochemically relevant redox reactions that does not require enzymatic catalysis, so thiol-disulfide redox potential is the first for which fluorescent indicators have become available. They consist of YFP<sup>192</sup> or GFP mutants<sup>70,71</sup> bearing two cysteines on adjacent strands of the  $\beta$ -barrel, placed so that formation of the intramolecular disulfide linkage favors protonation of the FP chromophore. Such protonation quenches the fluorescence of the YFP but enhances the 390 to 400 nm excitation peak of the GFP at the expense of the 470 to 490 nm peak. Thus, the YFP-based indicator (rxYFP) is intensity-only, whereas the GFP-based indicators (roGFPs) are ratiometric in excitation. As expected from electrostatic effects, placement of positive charges near the cysteines speeds the reaction kinetics and makes the midpoint potentials more oxidizing.<sup>193,194</sup> Equilibration of rxYFP with oxidized/reduced glutathione (GSSG/GSH) is strongly catalyzed by glutaredoxin, so fusion of rxYFP with glutaredoxin makes the chimera kinetically specific for glutathione redox status.<sup>195</sup> The FP-based indicators allow continuous nondestructive monitoring of thiol-disulfide ratios in single cells or subcellular compartments and indicate that cytosol and mitochondria are much more reducing<sup>70,196</sup> than deduced from previous destructive measurements of GSH and GSSG. Although GSH is relatively easy to assay destructively, GSSG is equally important, yet far scarcer in cells and more difficult to assay because GSH must first be destroyed; also, much of GSSG may be compartmentalized and releasable only upon cell disruption.

The above thiol-disulfide redox indicators can indirectly respond to reactive oxygen species, especially when the latter are grossly elevated, but the linkages are complex and biologically interesting in their own right. Therefore, indicators specific for individual reactive oxygen and nitrogen species would be valuable. Small-molecule fluorescent sensors for  $H_2O_2$  have been created by exploiting the ability of  $H_2O_2$  to convert

arylboronic acids into phenols and have now been able to detect phagocytosis-associated  $H_2O_2$  production in macrophages.<sup>197</sup> The first genetically encoded  $H_2O_2$  indicator is HyPer,<sup>72</sup> in which a circularly permuted YFP has been inserted into the regulatory domain of a prokaryotic  $H_2O_2$  sensor. This molecule has detected the much smaller  $H_2O_2$  transients associated with apoptotic and growth factor stimuli. Quenched fluorescein and rhodamine dyes that brighten upon reaction with singlet oxygen<sup>198</sup> or other highly reactive oxygen species (hydroxyl radical, peroxynitrite, and hypochlorite<sup>199,200</sup>) have been described, though minimal biological results have been reported yet. GFPs that respond specifically and irreversibly to singlet oxygen with an excitation ratio change have been developed (C. Dooley and R.Y. Tsien, unpublished). For signals related to nitric oxide (NO), one should distinguish between the free radical NO versus derivatives of the nitrosyl cation  $NO^+$ . A genetically encoded sensor for NO was based<sup>201</sup> on fusing GFP to the heme-binding region of soluble guanylyl cyclase, which presumably becomes loaded with endogenous heme. Exposure to NO irreversibly increased the GFP fluorescence by 14%, so this chimera is an integrator of NO exposure, not a reversible indicator of instantaneous levels. This indicator revealed the limited spatial spread and frequency dependence of NO generation from cerebellar synapses from parallel fibers onto Purkinje neurons.<sup>201</sup>  $NO^+$  can react with both thiols and aromatic amines instead of heme iron. Small-molecule dyes (fluoresceins and near-IR cyanines) containing o-phenylenediamines respond to  $NO^+$  by forming triazoles, preventing photo-induced electron transfer as described in section "Sequestration of Critical Lone Pair of Electrons" and thereby dequenching fluorescence.<sup>202</sup> The multiple cysteines in metallothioneins have been the basis for a genetically encoded FRET sensor for nitrosating species, such as nitrosothiols.<sup>203</sup>

### Endoprotease Activities

It is easier to deliver fluorescent or fluorogenic substrates to proteases that are extracellular or in the lumen of endocytic organelles than to proteases in other intracellular locations. Therefore, the former class of protease activities can be monitored by fluorescent suicide substrates (for mechanism see section "Fluorophore as Spectroscopically Passive Tag for Macromolecule of Interest"), release of free amines and lone pair electrons (see section "Sequestration of Critical Lone Pair of Electrons"), dequenching due to disaggregation (see section "Modulating of Quenching by Dye Aggregation"), disruption of

FRET (see section "FRET"), and activation of cell-penetrating peptides (see section "Activatable Cell-Penetrating Peptides"), whereas cytosolic endoprotease activities are most cleanly imaged by disruption of FRET between FPs. Proteases whose specificity is governed mainly by the amino acids on the acyl side of the peptide bond to be cleaved (the S1, S2, S3... positions) can be assayed destructively with a suicide substrate (...S3-S2-S1-warhead) or nondestructively with a cleavable substrate (...S3-S2-S1-dye). Attack of the active-site serine or cysteine on the warhead results in covalent labeling and inactivation of the enzyme.<sup>204,205</sup> The fragment that remains attached to the enzyme carries a fluorescent tag. If a portion of the warhead is displaced by the active-site serine or cysteine, the leaving group could carry a quencher, so that the fluorescence is quenched upon successful reaction with the enzyme.<sup>205</sup> This mechanism facilitates molecular identification of the relevant proteases, but it is most suited to serine or cysteine proteases, sacrifices enzymatic amplification, and potentially perturbs any biology downstream of the active protease. In cleavable substrates, hydrolysis of the amide bond between S1 and dye releases the free amine form of the latter, including the lone pair of electrons on the amine nitrogen. The dye is typically an aminocoumarin or aminoxanthene, in which the delocalization of the lone pair of electrons into the rest of the chromophore increases the intensity and the wavelength of the fluorescence compared with the intact substrate. Mechanisms described in sections "Modulating of Quenching by Dye Aggregation," "FRET," and "Activatable Cell-Penetrating Peptides," accommodate natural amino acids on the amine side of the peptide bond to be cleaved (the S1', S2', S3'... positions etc) and are equally applicable to all four major classes of proteases (serine, cysteine, aspartic, and metallo-). For these mechanisms, the cleavable peptides respectively link multiple fluorescent dyes to a polymeric backbone (see section "Modulating of Quenching by Dye Aggregation"), or donor to acceptor fluorophores (see section "FRET"), or polycationic to polyanionic sequences (see section "Activatable Cell-Penetrating Peptides"). Inside cells, FPs are usually the most convenient fluorophores, which are very easy to genetically combine into donor-linker-acceptor chimeras. Fortunately, the FPs themselves are generally quite resistant to endoproteases and proteolytic cleavage of the linker allows the donor and acceptor to diffuse apart, so that the FRET decrease is maximal. Caspase activation in apoptosis is a particularly popular application, where imaging readily reveals that the gradual response seen in cell populations is actually composed of transitions that are step-like in each individual cell but desynchronized between neighboring cells.<sup>206</sup>

### Ubiquitination and Proteasomal Degradation, Especially of Cell Cycle Proteins

Decoration of a protein by ubiquitin is a crucial signal to trigger degradation of that protein in proteasomes. Such ubiquitination has been imaged by FRET from a degradation-prone GFP to a YFP-ubiquitin fusion, which is evidently accepted by the ubiquitination machinery. The YFP had been mutated to reduce its emission quantum yield to near zero, whereas its absorbance was kept high to preserve its ability to accept FRET and thereby reduce the fluorescence lifetime of the GFP donor.<sup>207</sup>

The final degradation of the polyubiquitinated protein in proteasomes leads to destruction of any fused FP. Surprisingly, FPs seem to vary significantly in their resistance to such degradation. Relatively degradable green and orange-red FPs have been fused to geminin and Cdt1, nuclear proteins that respectively accumulate in S/G<sub>2</sub>/M and G<sub>1</sub> phases before being destroyed in late M/G<sub>1</sub> versus S/G<sub>2</sub> phases of the cell cycle. Therefore, in cells transfected with both constructs, nuclei in S/G<sub>2</sub>/M phase glow green, whereas nuclei in G<sub>1</sub> are scarlet. This combination enables visualization and tracking of the mitotic status of every cell in a culture, xenograft, or transgenic mammal.<sup>208</sup>

### Kinase and Phosphatase Activities

The most robust fluorescence reporters of the balance between endogenous protein kinases and phosphatases are chimeras in which donor and acceptor FPs bracket a linker containing a peptide substrate for phosphorylation/dephosphorylation and a protein domain that binds the relevant phosphorylated amino acid, for example, an SH2 domain for phosphotyrosine or an FHA1 domain for phosphothreonine. When the substrate becomes phosphorylated, it presumably is captured by the neighboring domain in some way like the folding of a jackknife. This conformational change can either increase or decrease FRET between the flanking FPs; either direction is acceptable provided that the change is sufficiently large and reproducible. The design and application of kinase activity reporters has been recently reviewed.<sup>209</sup> The specificity for particular protein kinases is governed by the substrate sequence and optional subcellular targeting. If the phosphorylation-recognizing domain has too high an affinity for the phosphorylated amino acid, it may protect the latter so thoroughly that phosphatases cannot attack, rendering the indicator irreversible.<sup>210</sup> Most kinase activity reporters are reversible, so they actually signal a balance between kinase and phosphatase activities, though we know comparatively little about which

phosphatases are involved. One phosphatase with a relatively well-defined role is calcineurin, which dephosphorylates and thereby activates an important family of transcription factors, the nuclear factors of activated T-cells (NFAT). Recently, a FRET sensor for calcineurin has been constructed<sup>211</sup> by sandwiching a truncated regulatory domain from NFAT1 between CFP and a circularly permuted YFP.

### Protein-Protein Interactions

The detection of protein-protein interactions is an enormous topic for which recent reviews should be consulted.<sup>94,212</sup> Please also see Chapter 47, "Molecular Imaging of Protein-Protein Interactions" for additional discussion. When the proteins of interest are fused either to donor and acceptor FPs or to fragments of FPs or of fluorogenic reporter enzymes, successful FRET or complementation (see sections "FRET" and "FP Complementation") give strong evidence for proximity within a few nanometers. However, a lack of observable FRET or complementation is usually not good evidence for lack of interaction, so these methods are best used to quantify the spatiotemporal dynamics of known interacting partners rather than as primary screens to find novel partners. For larger complexes where the distance between tags exceeds 10 nm, the best current approaches are probably to demonstrate that the tags remain colocalized even as they both diffuse randomly (fluorescence cross-correlation spectroscopy)<sup>213,214</sup> or as the spatial resolution is sharpened by single-molecule imaging.<sup>3,215,216</sup> Whereas most of the techniques described above require that the partners of interest be genetically fused and transfected, two-color super-resolution co-localization of antibodies should detect proximities of endogenous unfused proteins in histological sections.<sup>215</sup>

### SOME FUTURE PERSPECTIVES

The examples in section "Pathways Commonly Monitored by Fluorescence" suggest that FPs have been at the core of most new fluorescent sensors for biochemical pathways. Synthetic dyes and quantum dots have their individual domains of superiority, but the genetic encodability and targetability of FPs give them much wider applicability. The most direct route to translating the many FP-based sensors from tissue culture microscopy to whole-mouse imaging would be the development of bright FPs with excitation maxima above 600 nm to get past heme absorbances and minimize interference from autofluorescence. FRET partners or complementing fragments

working at such long wavelengths would be even more powerful (albeit challenging to create). High-quantum-yield FPs that are efficient BRET acceptors might provide alternatives in many cases (Chapter 22, "Nanochemistry for Molecular Imaging"). Further improvements in instruments and algorithms to collect and localize long-wavelength fluorescence from deep inside scattering tissues would be of complementary value, though beyond the scope of this review (Chapter 11, "Fluorescence Tomography," Chapter 14, "Diffuse Optical Tomography and Spectroscopy").

### REFERENCES

- Hell SW. Far-field optical nanoscopy. *Science* 2007;316:1153–8.
- Toprak E, Selvin PR. New fluorescent tools for watching nanometer-scale conformational changes of single molecules. *Annu Rev Biophys Biomol Struct* 2007;36:349–69.
- Michalet X, Lacoste TD, Weiss S. Ultrahigh-resolution colocalization of spectrally separable point-like fluorescent probes. *Methods* 2001;25:87–102.
- Park H, Toprak E, Selvin PR. Single-molecule fluorescence to study molecular motors. *Q Rev Biophys* 2007;40:87–111.
- Michalet X, Weiss S, Jager M. Single-molecule fluorescence studies of protein folding and conformational dynamics. *Chem Rev* 2006;106:1785–813.
- Lakowicz JR. *Principles of fluorescence spectroscopy*. New York: Springer; 2006.
- Schenke-Layland K, Riemann I, Damour O, et al. Two-photon microscopes and in vivo multiphoton tomographs—powerful diagnostic tools for tissue engineering and drug delivery. *Adv Drug Deliv Rev* 2006;58:878–96.
- Haugland RP. *Handbook of fluorescent probes and research chemicals*. Eugene (OR): Molecular Probes; 2002.
- Tsien RY. The green fluorescent protein. *Annu Rev Biochem* 1998;67:509–44.
- Shaner NC, Steinbach PA, Tsien RY. A guide to choosing fluorescent proteins. *Nat Methods* 2005;2:905–9.
- Lukyanov KA, Chudakov DM, Fradkov AF, et al. Discovery and properties of GFP-like proteins from nonbioluminescent anthozoa. *Methods Biochem Anal* 2006;47:121–38.
- Baird GS, Zacharias DA, Tsien RY. Biochemistry, mutagenesis, and oligomerization of dsRed, a red fluorescent protein from coral. *Proc Natl Acad Sci U S A* 2000;97:11984–9.
- Campbell RE, Tour O, Palmer AE, et al. A monomeric red fluorescent protein. *Proc Natl Acad Sci U S A* 2002;99:7877–82.
- Zhu H, Wang G, Li G, et al. Ubiquitous expression of mRFP1 in transgenic mice. *Genesis* 2005;42:86–90.
- Long JZ, Lackan CS, Hadjantonakis AK. Genetic and spectrally distinct in vivo imaging: embryonic stem cells and mice with widespread expression of a monomeric red fluorescent protein. *BMC Biotechnol* 2005;5:20.
- Shuen JA, Chen M, Gloss B, Calakos N. Drd1a-tdTomato BAC transgenic mice for simultaneous visualization of medium spiny neurons in the direct and indirect pathways of the basal ganglia. *J Neurosci* 2008;28:2681–5.
- Shaner NC, Campbell RE, Steinbach PA, et al. Improved monomeric red, orange and yellow fluorescent proteins derived from *Discosoma* sp. red fluorescent protein. *Nat Biotechnol* 2004;22:1567–72.
- Merzlyak EM, Goedhart J, Scherbo D, et al. Bright monomeric red fluorescent protein with an extended fluorescence lifetime. *Nat Methods* 2007;4:555–7.



## 824 MOLECULAR IMAGING: PRINCIPLES AND PRACTICE

19. Phillips GN. Structure and dynamics of green fluorescent protein. *Curr Opin Struct Biol* 1999;7:821–7.
20. Zacharias DA, Violin JD, Newton AC, Tsien RY. Partitioning of lipid-modified monomeric GFPs into membrane microdomains of live cells. *Science* 2002;296:913–6.
21. Zacharias DA. Sticky caveats in an otherwise glowing report: oligomerizing fluorescent proteins and their use in cell biology. *Sci STKE* 2002;2002:PE23.
22. Zhang L, Patel HN, Lappe JW, Wachter RM. Reaction progress of chromophore biogenesis in green fluorescent protein. *J Am Chem Soc* 2006;128:4766–72.
23. Wiedenmann J, Elke C, Spindler KD, Funke W. Cracks in the beta-can: fluorescent proteins from *Anemonia sulcata* Anthozoa, Actinaria). *Proc Natl Acad Sci U S A* 2002;99:13358.
24. Hansen MC, Palmer RJ Jr, Udsen C, et al. Assessment of GFP fluorescence in cells of *Streptococcus gordonii* under conditions of low pH and low oxygen concentration. *Microbiology* 2001;147:1383–91.
25. Zhang C, Xing XH, Lou K. Rapid detection of a *gfp*-marked *Enterobacter aerogenes* under anaerobic conditions by aerobic fluorescence recovery. *FEMS Microbiol Lett* 2005;249:211–8.
26. Meyer T, Teruel MN. Fluorescence imaging of signaling networks. *Trends Cell Biol* 2003;13:101–6.
27. O'Rourke NA, Meyer T, Chandy G. Protein localization studies in the age of 'Omics'. *Curr Opin Chem Biol* 2005;9:82–7.
28. Chen I, Ting AY. Site-specific labeling of proteins with small molecules in live cells. *Curr Opin Biotechnol* 2005;16:35–40.
29. O'Hare HM, Johnsson K, Gautier A. Chemical probes shed light on protein function. *Curr Opin Struct Biol* 2007;17:488–94.
30. Wang L, Xie J, Schultz PG. Expanding the genetic code. *Annu Rev Biophys Biomol Struct* 2006;35:225–49.
31. Griffin BA, Adams SR, Tsien RY. Specific covalent labeling of recombinant protein molecules inside live cells. *Science* 1998;281:269–72.
32. Martin BR, Giepmans BN, Adams SR, Tsien RY. Mammalian cell-based optimization of the biarsenical-binding tetracysteine motif for improved fluorescence and affinity. *Nat Biotechnol* 2005;23:1308–14.
33. Rice MC, Czymmek K, Kmiec EB. The potential of nucleic acid repair in functional genomics. *Nat Biotechnol* 2001;19:321–6.
34. Rodriguez AJ, Shenoy SM, Singer RH, Condeelis J. Visualization of mRNA translation in living cells. *J Cell Biol* 2006;175:67–76.
35. Gaietta G, Deerinck TJ, Adams SR, et al. Multicolor and electron microscopic imaging of connexin trafficking. *Science* 2002;296:503–7.
36. Ju W, Morishita W, Tsui J, et al. Activity-dependent regulation of dendritic synthesis and trafficking of AMPA receptors. *Nat Neurosci* 2004;7:244–53.
37. Gaietta GM, Giepmans BN, Deerinck TJ, et al. Golgi twins in late mitosis revealed by genetically encoded tags for live cell imaging and correlated electron microscopy. *Proc Natl Acad Sci U S A* 2006;103:17777–82.
38. Tour O, Meijer RM, Zacharias DA, et al. Genetically targeted chromophore-assisted light inactivation. *Nat Biotechnol* 2003;21:1505–8.
39. Ignatova Z, Gierasch LM. Monitoring protein stability and aggregation in vivo by real-time fluorescent labeling. *Proc Natl Acad Sci U S A* 2004;101:523–8.
40. Guignet EG, Hovius R, Vogel H. Reversible site-selective labeling of membrane proteins in live cells. *Nat Biotechnol* 2004;22:440–4.
41. Kapanidis AN, Ebricht YW, Ebricht RH. Site-specific incorporation of fluorescent probes into protein: hexahistidine-tag-mediated fluorescent labeling with (Ni<sup>2+</sup>): nitrilotriacetic Acid (n)-fluorochrome conjugates. *J Am Chem Soc* 2001;123:12123–5.
42. Hauser CT, Tsien RY. A hexahistidine-Zn<sup>2+</sup>-dye label reveals STIM1 surface exposure. *Proc Natl Acad Sci U S A* 2007;104:3693–7.
43. Fernandez-Suarez M, Baruah H, Martinez-Hernandez L, et al. Redirecting lipoic acid ligase for cell surface protein labeling with small-molecule probes. *Nat Biotechnol* 2007;25:1483–7.
44. Howarth M, Takao K, Hayashi Y, Ting AY. Targeting quantum dots to surface proteins in living cells with biotin ligase. *Proc Natl Acad Sci U S A* 2005;102:7583–8.
45. Slavoff SA, Chen I, Choi YA, Ting AY. Expanding the substrate tolerance of biotin ligase through exploration of enzymes from diverse species. *J Am Chem Soc* 2008;130:1160–2.
46. Mao H, Hart SA, Schink A, Pollok BA. Sortase-mediated protein ligation: a new method for protein engineering. *J Am Chem Soc* 2004;126:2670–1.
47. Gautier A, Juillerat A, Heinis C, et al. An engineered protein tag for multiprotein labeling in living cells. *Chem Biol* 2008;15:128–36.
48. Szent-Gyorgyi C, Schmidt BA, Creeger Y, et al. Fluorogen-activating single-chain antibodies for imaging cell surface proteins. *Nat Biotechnol* 2008;26:235–40.
49. Fischer AJ, Lagarias JC. Harnessing phytochrome's glowing potential. *Proc Natl Acad Sci U S A* 2004;101:17334–9.
50. Murphy JT, Lagarias JC. The phytofluors: a new class of fluorescent protein probes. *Curr Biol* 1997;7:870–6.
51. Shu X, Royant A, Lin MZ, Aguilera TA, Lev-Ram V, Steinbach PA, Tsien RY. Mammalian expression of infrared fluorescent proteins engineered from a bacterial phytochrome. *Science* 2009, in press.
52. Adams SR. How calcium indicators work. In *Imaging in Neuroscience and Development*. eds. Yuste R, & Konnerth A. (Cold Spring Harbor: Cold Spring Harbor Laboratory Press), 2005; pp. 239–44.
53. Kao JPY, Harootyanian AT, Tsien RY. Photochemically generated cytosolic calcium pulses and their detection by fluo-3. *J Biol Chem* 1989;264:8179–84.
54. Lakowicz JR, Szymanski H, Johnson ML. Calcium imaging using fluorescence lifetimes and long-wavelength probes. *J Fluoresc* 1992;2:47–62.
55. Mason SF. Color and the electronic state of organic molecules. In: Venkataraman K, editor. *The chemistry of synthetic dyes*. Vol III. New York: Academic Press; 1970. p. 169–221.
56. Zhuang X, Ha T, Kim HD, et al. Fluorescence quenching: a tool for single-molecule protein-folding study. *Proc Natl Acad Sci U S A* 2000;97:14241–4.
57. Blumenthal R, Gallo SA, Viard M, et al. Fluorescent lipid probes in the study of viral membrane fusion. *Chem Phys Lipids* 2002;116:39–55.
58. Bremer C, Bredow S, Mahmood U, et al. Optical imaging of matrix metalloproteinase-2 activity in tumors: feasibility study in a mouse model. *Radiology* 2001;221:523–9.
59. Bremer C, Tung CH, Weissleder R. In vivo molecular target assessment of matrix metalloproteinase inhibition. *Nat Med* 2001;7:743–8.
60. Funovics M, Weissleder R, Tung CH. Protease sensors for bioimaging. *Anal Bioanal Chem* 2003;377:956–63.
61. Mahmood U, Weissleder R. Near-infrared optical imaging of proteases in cancer. *Mol Cancer Ther* 2003;2:489–96.
62. Hama Y, Urano Y, Koyama Y, et al. A target cell-specific activatable fluorescence probe for in vivo molecular imaging of cancer based on a self-quenched avidin-rhodamine conjugate. *Cancer Res* 2007;67:2791–9.
63. Brejc K, Sixma TK, Kitts PA, et al. Structural basis for dual excitation and photoisomerization of the *Aequorea victoria* green fluorescent protein. *Proc Natl Acad Sci U S A* 1997;94:2306–11.
64. Ward WW, Prentice HJ, Roth AF, et al. Spectral perturbations of the *Aequorea* green-fluorescent protein. *Photochem Photobiol* 1982;35:803–8.
65. Chattoraj M, King BA, Bublitz GU, Boxer SG. Ultra-fast excited state dynamics in green fluorescent protein: multiple states and proton transfer. *Proc Natl Acad Sci U S A* 1996;93:8362–7.
66. Tsien RY, Prasher DC. Molecular biology and mutation of GFP. In: Chalfie M, Kain S, editors. *GFP: green fluorescent protein strategies and applications*. New York: Wiley & Sons; 1998. pp. 97–118

67. Llopis J, McCaffery JM, Miyawaki A, et al. Measurement of cytosolic, mitochondrial and golgi pH in single living cells with green fluorescent protein. *Proc Natl Acad Sci U S A* 1998;95:6803–8.
68. Yuste R, Miller RA, Holthoff K, et al. Synapto-pHluorins: chimeras between pH-sensitive mutants of green fluorescent protein and synaptic vesicle membrane proteins as reporters of neurotransmitter release. *Methods Enzymol* 2000;327:522–46.
69. Jayaraman S, Haggie P, Wachter RM, et al. Mechanism and cellular applications of a green fluorescent protein-based halide sensor. *J Biol Chem* 2000;275:6047–50.
70. Dooley CM, Dore TM, Hanson GT, et al. Imaging dynamic redox changes in mammalian cells with green fluorescent protein indicators. *J Biol Chem* 2004;279:22284–93.
71. Hanson GT, Aggeler R, Oglesbe D, et al. Investigating mitochondrial redox potential with redox-sensitive green fluorescent protein indicators. *J Biol Chem* 2004;279:13044–53.
72. Belousov VV, Fradkov AF, Lukyanov KA, et al. Genetically encoded fluorescent indicator for intracellular hydrogen peroxide. *Nat Methods* 2006;3:281–6.
73. Baird GS, Zacharias DA, Tsien RY. Circular permutation and receptor insertion within green fluorescent proteins. *Proc Natl Acad Sci U S A* 1999;96:11241–6.
74. Nagai T, Sawano A, Park E, Miyawaki A. Circularly permuted green fluorescent proteins engineered to sense Ca<sup>2+</sup>. *Proc Natl Acad Sci U S A* 2001;98:3197–202.
75. Nakai J, Ohkura M, Imoto K. A high signal-to-noise Ca<sup>2+</sup> probe composed of a single green fluorescent protein. *Nat Biotechnol* 2001;19:137–41.
76. Mao T, O'Connor DH, Scheuss V, et al. Characterization and subcellular targeting of GCaMP-type genetically encoded calcium indicators. *PLoS ONE* 2008;3:e1796.
77. Ohkura M, Matsuzaki M, Kasai H, et al. Genetically encoded bright Ca<sup>2+</sup> probe applicable for dynamic Ca<sup>2+</sup> imaging of dendritic spines. *Anal Chem* 2005;77:5861–9.
78. Reiff DF, Ihring A, Guerrero G, et al. In vivo performance of genetically encoded indicators of neural activity in flies. *J Neurosci* 2005;25:4766–78.
79. Guerrero G, Siegel MS, Roska B, et al. Tuning FlaSh: redesign of the dynamics, voltage range, and color of the genetically encoded optical sensor of membrane potential. *Biophys J* 2002;83:3607–18.
80. Piston DW, Kremers GJ. Fluorescent protein FRET: the good, the bad and the ugly. *Trends Biochem Sci* 2007;32:407–14.
81. Tsien RY. Indicators based on fluorescence resonance energy transfer. In: Yuste R, Konnerth A, editors. *Imaging in neuroscience and development*. Cold Spring Harbor: Cold Spring Harbor Laboratory Press; 2005. p. 549–56.
82. Jovin TM, Arndt-Jovin DJ. Luminescence digital imaging microscopy. *Annu Rev Biophys Chem* 1989;18:271–308.
83. Gordon GW, Berry G, Liang XH, et al. Quantitative fluorescence resonance energy transfer measurements using fluorescence microscopy. *Biophys J* 1998;74:2702–13.
84. Sorkin A, McClure M, Huang F, Carter R. Interaction of EGF receptor and grb2 in living cells visualized by fluorescence resonance energy transfer (FRET) microscopy. *Curr Biol* 2000;10:1395–8.
85. Erickson MG, Alseikhan BA, Peterson BZ, Yue DT. Preassociation of calmodulin with voltage-gated Ca(2+) channels revealed by FRET in single living cells. *Neuron* 2001;31:973–85.
86. Miyawaki A, Tsien RY. Monitoring protein conformations and interactions by fluorescence resonance energy transfer between mutants of green fluorescent protein. *Methods Enzymol* 2000;327:472–500.
87. Bastiaens PI, Squire A. Fluorescence lifetime imaging microscopy: spatial resolution of biochemical processes in the cell. *Trends Cell Biol* 1999;9:48–52.
88. Tramier M, Coppey-Moisan M. Fluorescence anisotropy imaging microscopy for homo-FRET in living cells. *Methods Cell Biol* 2008;85:395–414.
89. Nagai T, Yamada S, Tominaga T, et al. Expanded dynamic range of fluorescent indicators for Ca(2+) by circularly permuted yellow fluorescent proteins. *Proc Natl Acad Sci U S A* 2004;101:10554–9.
90. Hamdan FF, Percherancier Y, Breton B, Bouvier M. Monitoring protein-protein interactions in living cells by bioluminescence resonance energy transfer (BRET). *Curr Protoc Neurosci* 2006, Chapter 5, unit 5.23.
91. Bacart J, Corbel C, Jockers R, et al. The BRET technology and its application to screening assays. *Biotechnol J* 2008;3:311–24.
92. Massoud TF, Paulmurugan R, De A, et al. Reporter gene imaging of protein-protein interactions in living subjects. *Curr Opin Biotechnol* 2007;18:31–7.
93. Michnick SW, Ear PH, Manderson EN, et al. Universal strategies in research and drug discovery based on protein-fragment complementation assays. *Nat Rev Drug Discov* 2007;6:569–82.
94. Villalobos V, Naik S, Piwnicka-Worms D. Current state of imaging protein-protein interactions in vivo with genetically encoded reporters. *Annu Rev Biomed Eng* 2007;9:321–49.
95. Ghosh I, Hamilton AD, Regan L. Antiparallel leucine zipper-directed protein reassembly: application to the green fluorescent protein. *J Am Chem Soc* 2000;122:5658–9.
96. Hu C-D, Chinenov Y, Kerppola TK. Visualization of interactions among bZIP and Rel family proteins in living cells using bimolecular fluorescence complementation. *Mol Cell* 2002;9:789–98.
97. Zhang S, Ma C, Chalfie M. Combinatorial marking of cells and organelles with reconstituted fluorescent proteins. *Cell* 2004;119:137–44.
98. Hu CD, Kerppola TK. Simultaneous visualization of multiple protein interactions in living cells using multicolor fluorescence complementation analysis. *Nat Biotechnol* 2003;21:539–45.
99. Cabantous S, Terwilliger TC, Waldo GS. Protein tagging and detection with engineered self-assembling fragments of green fluorescent protein. *Nat Biotechnol* 2005;23:102–7.
100. Langel U, editor. *Handbook of cell-penetrating peptides*. Boca Raton (FL): Taylor and Francis; 2007.
101. Jiang T, Olson ES, Nguyen QT, et al. Tumor imaging by means of proteolytic activation of cell-penetrating peptides. *Proc Natl Acad Sci U S A* 2004;101:17867–72.
102. Goun EA, Shinde R, Dehnert KW, et al. Intracellular cargo delivery by an octaarginine transporter adapted to target prostate cancer cells through cell surface protease activation. *Bioconjug Chem* 2006;17:787–96.
103. Zhang Y, So MK, Rao J. Protease-modulated cellular uptake of quantum dots. *Nano Lett* 2006;6:1988–92.
104. Olson ES, Jiang T, Scadeng M, Ellies LG, Nguyen QT, Aguilera TA, Tsien RY. ACPPs attached to dendrimeric nanoparticles: development of dual probes for fluorescence and magnetic resonance imaging of proteases in vivo.
105. Whitney M, Olson ES, Aguilera TA, Crisp JL, Gross LA, Ellies LG, Tsien RY. Parallel in vivo and in vitro selection using phage display identifies protease dependent tumor targeting peptides.
106. Dolmetsch RE, Gomez-Ospina N, Green E, Nigh EA. Imaging gene expression in live cells and tissues. In: Yuste R, Konnerth A, editors. *Imaging in neuroscience and development*. Cold Spring Harbor: Cold Spring Harbor Laboratory Press; 2005. p. 605–17.
107. Chalfie M, Tu Y, Euskirchen G, et al. Green fluorescent protein as a marker for gene expression. *Science* 1994;263:802–5.
108. Barth AL. Visualizing circuits and systems using transgenic reporters of neural activity. *Curr Opin Neurobiol* 2007;17:567–71.
109. Yu J, Xiao J, Ren X, et al. Probing gene expression in live cells, one protein molecule at a time. *Science* 2006;311:1600–3.
110. Li X, Zhao X, Fang Y, et al. Generation of destabilized green fluorescent protein as a transcription reporter. *J Biol Chem* 1998;273:34970–5.

111. Dantuma NP, Lindsten K, Glas R, et al. Short-lived green fluorescent proteins for quantifying ubiquitin/proteasome-dependent proteolysis in living cells. *Nat Biotechnol* 2000;18:538–43.
112. Lichtman JW, Livet J, Sanes JR. A technicolour approach to the connectome. *Nat Rev Neurosci* 2008;9:417–22.
113. Livet J, Weissman TA, Kang H, et al. Transgenic strategies for combinatorial expression of fluorescent proteins in the nervous system. *Nature* 2007;450:56–62.
114. Babendure JR, Babendure JL, Ding JH, Tsien RY. Control of mammalian translation by mRNA structure near caps. *RNA* 2006;12:851–61.
115. Bouabe H, Fassler R, Heesemann J. Improvement of reporter activity by IRES-mediated polycistronic reporter system. *Nucleic Acids Res* 2008;36:e28.
116. Weinberger LS, Burnett JC, Toettcher JE, et al. Stochastic gene expression in a lentiviral positive-feedback loop: HIV-1 Tat fluctuations drive phenotypic diversity. *Cell* 2005;122:169–82.
117. Straight AF, Marshall WF, Sedat JW, Murray AW. Mitosis in living budding yeast: anaphase A but no metaphase plate. *Science* 1997;277:574–8.
118. Kumaran RI, Spector DL. A genetic locus targeted to the nuclear periphery in living cells maintains its transcriptional competence. *J Cell Biol* 2008;180:51–65.
119. Querido E, Chartrand P. Using fluorescent proteins to study mRNA trafficking in living cells. *Methods Cell Biol* 2008;85:273–92.
120. Elf J, Li GW, Xie XS. Probing transcription factor dynamics at the single-molecule level in a living cell. *Science* 2007;316:1191–4.
121. Daunert S, Barrett G, Feliciano JS, et al. Genetically engineered whole-cell sensing systems: coupling biological recognition with reporter genes. *Chem Rev* 2000;100:2705–38.
122. Huang Z, Terpetschnig E, You W, Haugland RP. 2-(2'-Phosphoroxoxyphenyl)-4(3*H*)-quinazolinone derivatives as fluorogenic precipitating substrates of phosphatases. *Anal Biochem* 1992;207:32–9.
123. Kamiya M, Kobayashi H, Hama Y, et al. An enzymatically activated fluorescence probe for targeted tumor imaging. *J Am Chem Soc* 2007;129:3918–29.
124. Zlokarnik G, Negulescu PA, Knapp TE, et al. Quantitation of transcription and clonal selection of single living cells using  $\beta$ -lactamase as reporter. *Science* 1998;279:84–8.
125. Wildt S, Deuschle U. *cobA*, a red fluorescent transcriptional reporter for *Escherichia coli*, yeast, and mammalian cells. *Nat Biotechnol* 1999;17:1175–8.
126. Knapp T, Hare E, Feng L, et al. Detection of beta-lactamase reporter gene expression by flow cytometry. *Cytometry* 2003;51A:68–78.
127. Raz E, Zlokarnik G, Tsien RY, Driever W. Beta-Lactamase as a marker for gene expression in live zebrafish embryos. *Dev Biol* 1998;203:290–4.
128. Wolff M, Wiedenmann J, Nienhaus GU, et al. Novel fluorescent proteins for high-content screening. *Drug Discov Today* 2006;11:1054–60.
129. Terskikh A, Fradkov A, Ermakova G, et al. "Fluorescent timer": protein that changes color with time. *Science* 2000;290:1585–8.
130. Verkhusha VV, Chudakov DM, Gurskaya NG, et al. Common pathway for the red chromophore formation in fluorescent proteins and chromoproteins. *Chem Biol* 2004;11:845–54.
131. Kaether C, Gerdes HH. Visualization of protein transport along the secretory pathway using green fluorescent protein. *FEBS Lett* 1995;369:267–71.
132. Lippincott-Schwartz J, Patterson GH. Fluorescent proteins for photoactivation experiments. *Methods Cell Biol* 2008;85:45–61.
133. Shaner NC, Patterson GH, Davidson MW. Advances in fluorescent protein technology. *J Cell Sci* 2007;120:4247–60.
134. Stark DA, Kulesa PM. An in vivo comparison of photoactivatable fluorescent proteins in an avian embryo model. *Dev Dyn* 2007;236:1583–94.
135. Baskin JM, Prescher JA, Laughlin ST, et al. Copper-free click chemistry for dynamic in vivo imaging. *Proc Natl Acad Sci U S A* 2007;104:16793–7.
136. Lin MZ, Glenn JS, Tsien RY. A drug-controllable tag for visualizing newly synthesized proteins in cells and whole animals. *Proc Natl Acad Sci U S A* 2008;105:7744–9.
137. Schweizer FE, Ryan TA. The synaptic vesicle: cycle of exocytosis and endocytosis. *Curr Opin Neurobiol* 2006;16:298–304.
138. Brumback AC, Lieber JL, Angleson JK, Betz WJ. Using FM1-43 to study neuropeptide granule dynamics and exocytosis. *Methods* 2004;33:287–94.
139. Miesenböck G. A practical guide: Synapto-pHluorins—Genetically encoded reporters of synaptic transmission. In: Yuste R, Konnerth A, editors. *Imaging in neuroscience and development*. Cold Spring Harbor: Cold Spring Harbor Laboratory Press; 2005. p. 599–603.
140. Bozza T, McGann JP, Mombaerts P, Wachowiak M. In vivo imaging of neuronal activity by targeted expression of a genetically encoded probe in the mouse. *Neuron* 2004;42:9–21.
141. Babendure JR, Adams SR, Tsien RY. Aptamers switch on fluorescence of triphenylmethane dyes. *J Am Chem Soc* 2003;125:14716–7.
142. Rackham O, Brown CM. Visualization of RNA-protein interactions in living cells: FMRP and IMP1 interact on mRNAs. *EMBO J* 2004;23:3346–55.
143. Tsien RY. Fluorescent indicators of ion concentrations. *Methods Cell Biol* 1989;30:127–56.
144. Miesenböck G, De Angelis DA, Rothman JE. Visualizing secretion and synaptic transmission with pH-sensitive green fluorescent proteins. *Nature* 1998;394:192–5.
145. McAnaney TB, Shi XH, Abbyad P, et al. Green fluorescent protein variants as ratiometric dual emission pH sensors. 3. Temperature dependence of proton transfer. *Biochemistry* 2005;44:8701–11.
146. Knopfel T, Diez-Garcia J, Akemann W. Optical probing of neuronal circuit dynamics: genetically encoded versus classical fluorescent sensors. *Trends Neurosci* 2006;29:160–6.
147. Ratto GM, Payne R, Owen WG, Tsien RY. The concentration of cytosolic free calcium in vertebrate rod outer segments measured with fura-2. *J Neurosci* 1988;8:3240–6.
148. Garaschuk O, Milos RI, Grienberger C, et al. Optical monitoring of brain function in vivo: from neurons to networks. *Pflugers Arch* 2006;453:385–96.
149. Ohki K, Chung S, Kara P, et al. Highly ordered arrangement of single neurons in orientation pinwheels. *Nature* 2006;442:925–8.
150. Tymianski M, Spigelman I, Zhang L, et al. Mechanism of action and persistence of neuroprotection by cell-permeant  $Ca^{2+}$  chelators. *J Cereb Blood Flow Metab* 1994;14:911–23.
151. Kotlikoff MI. Genetically encoded  $Ca^{2+}$  indicators: using genetics and molecular design to understand complex physiology. *J Physiol* 2007;578:55–67.
152. Palmer AE, Giacomello M, Kortemme T, et al. New  $Ca^{2+}$  indicators based on computationally-redesigned calmodulin-peptide pairs. *Chem Biol* 2006;13:521–30.
153. Garaschuk O, Griesbeck O, Konnerth A. Troponin C-based biosensors: a new family of genetically encoded indicators for in vivo calcium imaging in the nervous system. *Cell Calcium* 2007;42:351–61.
154. Tour O, Adams SR, Kerr RA, et al. Calcium Green FAsH as a genetically targeted small-molecule calcium indicator. *Nat Chem Biol* 2007;3:423–31.
155. Arslan P, Di Virgilio F, Beltrame M, et al. Cytosolic  $Ca^{2+}$  homeostasis in Ehrlich and Yoshida carcinomas. *J Biol Chem* 1985;260:2719–27.
156. Tomsig JL, Suszkiw JB.  $Pb^{2+}$ -induced secretion from bovine chromaffin cells: fura-2 as a probe for  $Pb^{2+}$ . *Am J Physiol* 1990;259:C762–8.

157. Hinkle PM, Shanshala EDI, Nelson EJ. Measurement of intracellular cadmium with fluorescent dyes. Further evidence for the role of calcium channels in cadmium uptake. *J Biol Chem* 1992; 267:25553–9.
158. Marchi B, Burlando B, Panfoli I, Viarengo A. Interference of heavy metal cations with fluorescent  $\text{Ca}^{2+}$  probes does not affect  $\text{Ca}^{2+}$  measurements in living cells. *Cell Calcium* 2000;28:225–31.
159. Atar D, Backx PH, Appel MM, et al. Excitation-transcription coupling mediated by zinc influx through voltage-dependent calcium channels. *J Biol Chem* 1995;270:2473–7.
160. Burdette SC, Walkup GK, Spingler, B, et al. New fluorescent sensors for  $\text{Zn}^{2+}$  based on a fluorescein platform: synthesis, properties and intracellular distribution. *J Am Chem Soc* 2001;123:7831–41.
161. Minta A, Tsien RY. Fluorescent indicators for cytosolic sodium. *J Biol Chem* 1989;264:19449–57.
162. Pearce LL, Gandle RE, Han W, et al. Role of metallothionein in nitric oxide signaling as revealed by a new green fluorescent fusion protein. *Proc Natl Acad Sci U S A* 2000;97:477–82.
163. Bozym RA, Thompson RB, Stoddard AK, Fierke CA. Measuring picomolar intracellular exchangeable zinc in PC-12 cells using a ratiometric fluorescence biosensor. *ACS Chem Biol* 2006; 1:103–11.
164. Evers TH, Appelhof MA, Graaf-Heuvelmans PT, et al. Ratiometric detection of Zn(II) using chelating fluorescent protein chimeras. *J Mol Biol* 2007;374:411–25.
165. van Dongen EM, Evers TH, Dekkers LM, et al. Variation of linker length in ratiometric fluorescent sensor proteins allows rational tuning of Zn(II) affinity in the picomolar to femtomolar range. *J Am Chem Soc* 2007;129:3494–5.
166. Biwersi J, Farah N, Wang Y-X, et al. Synthesis of cell-impermeable Cl<sup>-</sup>-sensitive fluorescent indicators with improved sensitivity and optical properties. *Am J Physiol* 1992;262:C243–50.
167. Verkman AS. Development and biological applications of chloride-sensitive fluorescent indicators. *Am J Physiol* 1990;259:C375–88.
168. Kuner T, Augustine GJ. A genetically encoded ratiometric indicator for chloride: capturing chloride transients in cultured hippocampal neurons. *Neuron* 2000;27:447–59.
169. Markova O, Mukhtarov M, Real E, et al. Genetically encoded chloride indicator with improved sensitivity. *J Neurosci Methods* 2008;170:67–76.
170. Gu H, Lalonde S, Okumoto S, et al. A novel analytical method for in vivo phosphate tracking. *FEBS Lett* 2006;580:5885–93.
171. Medintz IL. Recent progress in developing FRET-based intracellular sensors for the detection of small molecule nutrients and ligands. *Trends Biotechnol* 2006;24:539–42.
172. Hires SA, Zhu Y, Tsien RY. Optical measurement of synaptic glutamate spillover and reuptake by linker optimized glutamate-sensitive fluorescent reporters. *Proc Natl Acad Sci U S A* 2008; 105:4411–6.
173. Dulla C, Tani H, Okumoto S, et al. Imaging of glutamate in brain slices using FRET sensors. *J Neurosci Methods* 2008;168:306–19.
174. Lohse MJ, Bunemann M, Hoffmann C, et al. Monitoring receptor signaling by intramolecular FRET. *Curr Opin Pharmacol* 2007; 7:547–53.
175. Adams SR, Bacskai BJ, Taylor SS, Tsien RY. Optical probes for cyclic AMP. In: Mason WT, editor. *Fluorescent probes for biological activity of living cells — a practical guide*. New York: Academic Press; 1993. p. 133–49.
176. Bacskai BJ, Hochner B, Mahaut-Smith M, et al. Spatially resolved dynamics of cAMP and protein kinase A subunits in *Aplysia* sensory neurons. *Science* 1993;260:222–6.
177. Hempel CM, Vincent P, Adams SR, et al. Spatio-temporal dynamics of cAMP signals in an intact neural circuit. *Nature* 1996; 384:166–9.
178. Zaccolo M, De Giorgi F, Cho CY, et al. A genetically encoded, fluorescent indicator for cyclic AMP in living cells. *Nat Cell Biol* 2000;2:25–9.
179. Zaccolo M, Pozzan T. Discrete microdomains with high concentration of cAMP in stimulated rat neonatal cardiac myocytes. *Science* 2002;295:1711–5.
180. DiPilato LM, Cheng X, Zhang J. Fluorescent indicators of cAMP and Epac activation reveal differential dynamics of cAMP signaling within discrete subcellular compartments. *Proc Natl Acad Sci U S A* 2004;101:16513–8.
181. Nikolaev VO, Gambaryan S, Engelhardt S, et al. Real-time monitoring of the PDE2 activity of live cells: hormone-stimulated cAMP hydrolysis is faster than hormone-stimulated cAMP synthesis. *J Biol Chem* 2005;280:1716–9.
182. van der Krogt GN, Ogink J, Ponsioen B, Jalink K. A comparison of donor-acceptor pairs for genetically encoded FRET sensors: application to the Epac cAMP sensor as an example. *PLoS ONE* 2008;3:e1916.
183. Honda A, Adams SR, Sawyer CL, et al. Spatiotemporal dynamics of guanosine 3',5'-cyclic monophosphate revealed by a genetically encoded, fluorescent indicator. *Proc Natl Acad Sci U S A* 2001; 98:2437–42.
184. Nikolaev VO, Gambaryan S, Lohse MJ. Fluorescent sensors for rapid monitoring of intracellular cGMP. *Nat Methods* 2006;3:23–5.
185. Nausch LW, Ledoux J, Bonev AD, et al. Differential patterning of cGMP in vascular smooth muscle cells revealed by single GFP-linked biosensors. *Proc Natl Acad Sci U S A* 2008;105:365–70.
186. Matsu-ura T, Michikawa T, Inoue T, et al. Cytosolic inositol 1,4,5-trisphosphate dynamics during intracellular calcium oscillations in living cells. *J Cell Biol* 2006;173:755–65.
187. Murakoshi H, Iino R, Kobayashi T, et al. Single-molecule imaging analysis of Ras activation in living cells. *Proc Natl Acad Sci U S A* 2004;101:7317–22.
188. Bivona TG, Quatela S, Philips MR. Analysis of Ras activation in living cells with GFP-RBD. *Methods Enzymol* 2006;407:128–43.
189. Hodgson L, Pertz O, Hahn KM. Design and optimization of genetically encoded fluorescent biosensors: GTPase biosensors. *Methods Cell Biol* 2008;85:63–81.
190. Kitano M, Nakaya M, Nakamura T, et al. Imaging of Rab5 activity identifies essential regulators for phagosome maturation. *Nature* 2008;453:241–5.
191. Lohse MJ, Nikolaev VO, Hein P, et al. Optical techniques to analyze real-time activation and signaling of G-protein-coupled receptors. *Trends Pharmacol Sci* 2008;29:159–65.
192. Ostergaard H, Henriksen A, Hansen FG, Winther JR. Shedding light on disulfide bond formation: engineering a redox switch in green fluorescent protein. *EMBO J* 2001;20:5853–62.
193. Hansen RE, Ostergaard H, Winther JR. Increasing the reactivity of an artificial dithiol-disulfide pair through modification of the electrostatic milieu. *Biochemistry* 2005;44:5899–906.
194. Cannon MB, Remington SJ. Re-engineering redox-sensitive green fluorescent protein for improved response rate. *Protein Sci* 2006; 15:45–57.
195. Bjornberg O, Ostergaard H, Winther JR. Mechanistic insight provided by glutaredoxin within a fusion to redox-sensitive yellow fluorescent protein. *Biochemistry* 2006;45:2362–71.
196. Lopez-Mirabal HR, Winther JR. Redox characteristics of the eukaryotic cytosol. *Biochim Biophys Acta* 2008;1783:629–40.
197. Srikun D, Miller EW, Domaille DW, Chang CJ. An ICT-based approach to ratiometric fluorescence imaging of hydrogen peroxide produced in living cells. *J Am Chem Soc* 2008; 130:4596–7.
198. Tanaka K, Miura T, Umezawa N, et al. Rational design of fluorescein-based fluorescence probes. Mechanism-based design of a maximum fluorescence probe for singlet oxygen. *J Am Chem Soc* 2001;123:2530–6.
199. Kenmoku S, Urano Y, Kojima H, Nagano T. Development of a highly specific rhodamine-based fluorescence probe for hypochlorous acid and its application to real-time imaging of phagocytosis. *J Am Chem Soc* 2007;129:7313–8.

## 828 MOLECULAR IMAGING: PRINCIPLES AND PRACTICE

200. Koide Y, Urano Y, Kenmoku S, et al. Design and synthesis of fluorescent probes for selective detection of highly reactive oxygen species in mitochondria of living cells. *J Am Chem Soc* 2007;129:10324–5.
201. Namiki S, Kakizawa S, Hirose K, Iino M. No signalling decodes frequency of neuronal activity and generates synapse-specific plasticity in mouse cerebellum. *J Physiol* 2005;566:849–63.
202. Sasaki E, Kojima H, Nishimatsu H, et al. Highly sensitive near-infrared fluorescent probes for nitric oxide and their application to isolated organs. *J Am Chem Soc* 2005;127:3684–5.
203. St Croix CM, Stitt MS, Watkins SC, Pitt BR. Fluorescence resonance energy transfer-based assays for the real-time detection of nitric oxide signaling. *Methods Enzymol* 2005;396:317–26.
204. Cravatt BF, Wright AT, Kozarich JW. Activity-based protein profiling: from enzyme chemistry to proteomic chemistry. *Annu Rev Biochem* 2008;77:383–414.
205. Blum G, von Degenfeld G, Merchant MJ, et al. Noninvasive optical imaging of cysteine protease activity using fluorescently quenched activity-based probes. *Nat Chem Biol* 2007;3:668–77.
206. Rehm M, Dussmann H, Janicke RU, et al. Single-cell fluorescence resonance energy transfer analysis demonstrates that caspase activation during apoptosis is a rapid process. Role of caspase-3. *J Biol Chem* 2002;277:24506–14.
207. Ganesan S, Ameer-Beg SM, Ng TT, et al. A dark yellow fluorescent protein (YFP)-based Resonance Energy-Accepting Chromoprotein (REACH) for Förster resonance energy transfer with GFP. *Proc Natl Acad Sci U S A* 2006;103:4089–94.
208. Sakaue-Sawano A, Kurokawa H, Morimura T, et al. Visualizing spatiotemporal dynamics of multicellular cell-cycle progression. *Cell* 2008;132:487–98.
209. Zhang J, Allen MD. FRET-based biosensors for protein kinases: illuminating the kinome. *Mol Biosyst* 2007;3:759–65.
210. Zhang J, Hupfeld CJ, Taylor SS, et al. Insulin disrupts beta-adrenergic signalling to protein kinase A in adipocytes. *Nature* 2005;437:569–73.
211. Newman RH, Zhang J. Visualization of phosphatase activity in living cells with a FRET-based calcineurin activity sensor. *Mol Biosyst* 2008;4:496–501.
212. Lalonde S, Ehrhardt DW, Loque D, et al. Molecular and cellular approaches for the detection of protein-protein interactions: latest techniques and current limitations. *Plant J* 2008;53:610–35.
213. Briddon SJ, Hill SJ. Pharmacology under the microscope: the use of fluorescence correlation spectroscopy to determine the properties of ligand-receptor complexes. *Trends Pharmacol Sci* 2007;28:637–45.
214. Hausteiner E, Schwillke P. Fluorescence correlation spectroscopy: novel variations of an established technique. *Annu Rev Biophys Biomol Struct* 2007;36:151–69.
215. Bates M, Huang B, Dempsey GT, Zhuang X. Multicolor super-resolution imaging with photo-switchable fluorescent probes. *Science* 2007;317:1749–53.
216. Shroff H, Galbraith CG, Galbraith JA, et al. Dual-color superresolution imaging of genetically expressed probes within individual adhesion complexes. *Proc Natl Acad Sci U S A* 2007;104:20308–13.